NONCONFORMING IMMERSED FINITE ELEMENT METHODS FOR ELLIPTIC INTERFACE PROBLEMS

TAO LIN †, DONGWOO SHEEN‡, AND XU ZHANG§

arXiv:1510.00052v1 [math.NA] 30 Sep 2015

Abstract. New immersed finite element (IFE) methods are developed for second–order elliptic problems with discontinuous diffusion coefficient. IFE spaces are constructed based on the rotated–Q_1 nonconforming finite elements with the edge midpoint value and the edge mean value degrees of freedom. Approximation capability of these IFE spaces is analyzed by using appropriate interpolation operators and function spaces. The standard nonconforming Galerkin method is considered without any penalty stabilization term. Error estimates in energy– and L^2–norms are proved to be better than $O(h\sqrt{|\log h|})$ and $O(h^2|\log h|)$, respectively, where the $|\log h|$ factors reflect jump discontinuity. Numerical results are reported to confirm our analysis.

Key words. immersed finite element, nonconforming, rotated-Q_1, Cartesian mesh, elliptic interface problems

AMS subject classifications. 35R05, 65N15, 65N30

1. Introduction.

We consider the second-order elliptic interface problem:

$$-\nabla\cdot(\beta\nabla u) = f \quad \text{in } \Omega^-\cup\Omega^+, \tag{1.1a}$$

$$u = g \quad \text{on } \partial\Omega, \tag{1.1b}$$

where the physical domain $\Omega\subset\mathbb{R}^2$ is assumed to be formed by multiple materials. Without loss of generality, we assume that a C^2-continuous interface curve Γ separates the physical domain Ω into two sub-domains Ω^+ and Ω^-, such that $\overline{\Omega}=\overline{\Omega^+\cup\Omega^-\cup\Gamma}$ and $\Omega^-\Subset\Omega$. See an illustration in Figure 1.1. The diffusion coefficient $\beta(x,y)$ is discontinuous across the interface Γ, and it is assumed to be a piecewise constant function defined by

$$\beta(x,y)=\begin{cases}\beta^- & \text{if } (x,y)\in\Omega^-,\\ \beta^+ & \text{if } (x,y)\in\Omega^+,\end{cases} \tag{1.2}$$

such that $\min\{\beta^-,\beta^+\}>0$. Across the interface Γ, the solution and its flux are assumed to be continuous, *i.e.*,

$$[u]_\Gamma = 0, \tag{1.3a}$$

$$[\boldsymbol{\nu}\cdot\beta\nabla u]_\Gamma = 0, \tag{1.3b}$$

where $\boldsymbol{\nu}$ is the unit normal of Γ, and $[v]_\Gamma=v^+|_\Gamma-v^-|_\Gamma$.

Conventional finite element (FE) methods can solve this elliptic interface problem satisfactorily provided that solution meshes are shaped to fit the material interface [3]; otherwise the accuracy of the solution is uncertain [1]. *Immersed finite element* (IFE) methods [4, 9, 10, 11, 13, 18, 19, 21, 22, 23, 25, 28], on the other hand, do not require meshes to fit the interface. Hence, if desired, Cartesian meshes can be used

*This research was partially supported by the National Science Foundation (Grant Number DMS 1016313) and NRF–2014R1A2A1A11052429 in part.

†Department of Mathematics, Virginia Tech, Blacksburg, VA 24061, tlin@math.vt.edu

‡Department of Mathematics, and Interdisciplinary Program in Computational Science & Technology, Seoul National University, Seoul 08826, Korea, dongwoosheen@gmail.com

§Department of Mathematics, Purdue University, West Lafayette, IN 47907, xuzhang@purdue.edu

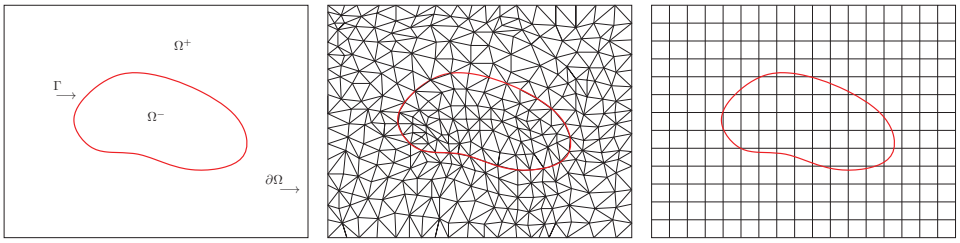

FIG. 1.1. *A geometry of interface problems. Body-fitting mesh and non-body-fitting mesh.*

to solve interface problems which is advantageous in many simulations. For example, in particle-in-cell methods for plasma particle simulations [14, 15], it is preferable to solve the governing electric potential interface problem on Cartesian meshes for efficient particle tracking. Also, IFE methods, in either a standard fully discrete or a semi discrete (the method of lines) formulation, can be used to solve time dependent problems with moving interfaces [12, 20] on a fixed Cartesian mesh throughout the whole simulation.

The fundamental idea of IFE methods (see e.g. [11, 19]), is to locally modify finite element functions on interface elements so that the interface jump conditions (1.3a) and (1.3b) are locally preserved in a certain sense. For elliptic interface problems, most of IFE methods in the literatures are adapted from the standard Lagrange type conforming FE spaces whose degrees of freedom are determined by nodal values in a mesh. However, IFE spaces originated from these conforming FE spaces are usually nonconforming because IFE functions are discontinuous across interface edges. This discontinuity can be harmfully large for certain configuration of interface location and diffusion coefficient. Consequently, the IFE solution is often less accurate around the interface than the rest of solution domain. Our recent numerical experiments reported in [21, 29] also indicate that the convergence rates of these conforming type IFE functions used in Galerkin formulation can deteriorate as the mesh size becomes very small.

New *partially penalized immersed finite element* (PPIFE) methods are introduced in [21, 29] to cope with the negative impacts caused by the discontinuity in IFE functions. In PPIFE schemes, penalization terms are added to IFE schemes which enables an enhance stability compared with classic IFE methods in the Galerkin formulation. The main idea of PPIFE arises from interior penalty discontinuous Galerkin (IPDG) methods [27]. However, in PPIFE methods, the stabilization terms are only added on interface edges compared to all interior edges for IPDG scheme [24]. With the enhanced stability enforced by the penalty over interface edges, these PPIFE schemes perform significantly better than classic IFE methods in the sense that errors around the interface are reduced notably and optimal convergence are observed in both L^2 and energy norms without deterioration on fine meshes. More importantly, *a priori* optimal error estimates can be theoretically establish for these schemes provided that the solution space has piecewise H^3 regularity (see [21]).

In this article, we develop a new class of IFE methods that uses an alternative approach to effectively alleviate the harmful impacts of discontinuity in IFE functions. In this new framework, the continuity of IFE function across element boundary is weakly enforced; hence there is no need to add penalty terms in the new scheme. Specifically, our new IFE spaces are based on nonconforming finite element spaces

[2, 6, 7, 16, 26] rather than conforming Lagrange type finite element spaces. One of the significant differences between conforming and nonconforming finite elements is how to enforce the continuity of finite element functions across elements. Conforming FE functions impose the continuity through nodal values at mesh points, while the continuity of nonconforming FE functions is imposed through mean values over edges. For IFE methods, an interface edge is cut by the interface into two pieces. The restriction of an IFE function to an interface edge leads to two piecewise polynomials from the two adjacent interface elements sharing this edge. In the conforming framework, these two piecewise polynomials coincide at the two endpoints of the interface edge, and this guarantees the continuity of the IFE function at the end nodes of the interface edge but not the whole interface edge. On the other hand, in the nonconforming framework, the continuity across an element edge is weakly enforced over the whole edge in the integral sense, no matter whether it is a polynomial or a piecewise polynomial. Thus we can take advantage of this nonconforming mechanism for constructing IFE functions that weakly preserve continuity over the whole of each interface edge.

The simplest nonconforming finite element defined on triangular meshes is the well-known Crouzeix-Raviart element [6]. For rectangular meshes, the simplest nonconforming finite elements are known as the *rotated-Q_1 finite elements* [2, 7, 16, 26]. Their degrees of freedom are determined either by values at midpoints of edges or by the integral values over edges. These two types of degrees of freedom coincide for Crouzeix-Raviart element. The Crouzeix-Raviart type IFE method has been discussed in [17]. In this article, we will develop new IFE spaces based on the rotated-Q_1 functions using both the midpoint-value and the integral-value degrees of freedom. As expected, the favored IFE space is the one with integral-value degrees of freedom because of it preserves continuity of approximating functions across element boundaries. This feature enables us to derive optimal error estimates for Galerkin IFE solution in both energy norm and L^2 norm.

The rest of this article is organized as follows. In Section 2, we construct the nonconforming rotated-Q_1 IFE spaces and present their basic properties. In Section 3, we discuss the approximation capabilities of these IFE spaces. In Section 4, we analyze errors of Galerkin solutions to the elliptic interface problem in energy and L^2 norms. In Section 5, numerical results are presented to confirm our analysis and demonstrate features of the new IFE methods. Finally, a few brief conclusions are provided in Section 6.

2. Nonconforming Immersed Finite Element Spaces. This section starts from notations and some preliminaries to be used in this paper. Then, it will introduce the nonconforming IFE spaces based on rotated-Q_1 elements.

2.1. Notations and Preliminaries. Multi-index notations will be employed such that $\alpha = (\alpha_1, \alpha_2) \in [\mathbb{Z}^+]^2$, $|\alpha| = \alpha_1 + \alpha_2$, together with the partial differential operator $\partial^\alpha = \frac{\partial^{\alpha_1}}{\partial x_1^{\alpha_1}} \frac{\partial^{\alpha_2}}{\partial x_2^{\alpha_2}}$, where $\mathbb{Z}^+$ denotes the set of all nonnegative integers. By $\widetilde{S}$ we denote the union of finite number of mutually disjoint open sets $S_j \subset \mathbb{R}^2, j = 1, \cdots, J$, and by S the interior of $\overline{\widetilde{S}}$, which contains $\widetilde{S}$ and all its possible interfaces. If $J = 1$, $\widetilde{S} = S$. Let $W^{m,p}(\widetilde{S})$ denote the usual Sobolev space with non-negative integer index m, equipped the norm and seminorm:

$$\|v\|_{m,p,\widetilde{S}} = \Big(\sum_{|\alpha| \le m} \int_{\widetilde{S}} |\partial^\alpha v(\mathbf{x})|^p \, \mathrm{dx} \Big)^{1/p}, \quad |v|_{m,p,\widetilde{S}} = \Big(\sum_{|\alpha| = m} \int_{\widetilde{S}} |\partial^\alpha v(\mathbf{x})|^p \, \mathrm{dx} \Big)^{1/p},$$

for $1 \le p < \infty$, and

$$\|v\|_{m,\infty,\widetilde{S}} = \max_{|\alpha|\le m} \operatorname{ess.sup}\{|v(x)| : \ x \in \widetilde{S}\}, \quad |v|_{m,\infty,\widetilde{S}} = \max_{|\alpha|=m} \operatorname{ess.sup}\{|v(x)| : \ x \in \widetilde{S}\}.$$

In particular, for $p = 2$, we denote $H^m(\widetilde{S}) = W^{m,p}(\widetilde{S})$, and we omit the index p in associated norms and seminorms for simplicity, *i.e.*, $\|v\|_{m,2,\widetilde{S}} = \|v\|_{m,\widetilde{S}}$, and $|v|_{m,2,\widetilde{S}} = |v|_{m,\widetilde{S}}$. We will also follow the convention to drop the domain index $\widetilde{S}$ if $\widetilde{S} = \Omega$. For $p = 2$, associated with the norm $\|\cdot\|_{m,\widetilde{S}}$, the inner product for $H^m(\widetilde{S})$ will be denoted by $(\cdot,\cdot)_{H^m(\widetilde{S})}$, with further simplification to $(\cdot,\cdot)_{\widetilde{S}}$ and $(\cdot,\cdot)$ if $m = 0$ and also if $\widetilde{S} = \Omega$, respectively.

For $m \ge 1$, we define two types of subspaces of $H^m(\widetilde{S})$ whose functions satisfy the interface jump conditions (1.3a) and (1.3b) on Γ. First, we set

$$\widetilde{H}^m_\Gamma(S) = H^1(S) \cap H^m(\widetilde{S}),$$

endowed with the inner-product and the norm

$$\langle u, v\rangle_{\widetilde{H}^m_\Gamma(S)} = (u,v)_{H^1(S)} + \sum_{j=1}^{J} \sum_{|\boldsymbol{\alpha}|=2} (\partial^{\boldsymbol{\alpha}} u, \partial^{\boldsymbol{\alpha}} v)_{L^2(S^j)}, \quad \|u\|_{\widetilde{H}^m_\Gamma(S)} = \sqrt{\langle u, u\rangle_{\widetilde{H}^m_\Gamma(S)}}.$$

Notice that $\widetilde{H}^1_\Gamma(S) = H^1(S)$ and that

$$[v]_\Gamma = 0 \text{ in the sense of } H^{\frac{1}{2}}(\Gamma) \quad \forall v \in \widetilde{H}^m_\Gamma(S), \ m \ge 1.$$

Finally, for $m = 2$, we define a subspace of $\widetilde{H}^m_\Gamma(S)$, which will be suitable for the analysis of interface problem, as follows:

$$\widetilde{H}^2_\beta(S) = \left\{ v \in \widetilde{H}^2_\Gamma(S) \mid \ [\![\boldsymbol{\nu}_\Gamma \cdot \beta \nabla u]\!]_\Gamma = 0 \right\}.$$

In addition, the following spaces will be useful: for $p \ge 2$,

$$\widetilde{W}^{2,p}_\Gamma(S) = W^{1,p}(S) \cap W^{2,p}(\widetilde{S}); \quad \widetilde{W}^{2,p}_\beta(S) = \{v \in \widetilde{W}^{2,p}_\beta(\Omega) \mid \ [\![\boldsymbol{\nu}_\Gamma \cdot \beta \nabla v]\!]_\Gamma = 0\}.$$

Here, and in what follows, $[v]_\Gamma$ and $[\![v]\!]_\Gamma$ will mean the jumps across Γ in the sense of $W^{1-\frac{1}{p},p}(\Gamma)$ and $W^{-\frac{1}{p},p}(\Gamma)$, respectively. However, if $u \in W^{2,p}(\widetilde{S})$, these jumps are defined in the sense of $W^{2-\frac{1}{p},p}(\Gamma)$ and $W^{1-\frac{1}{p},p}(\Gamma)$, respectively.

Assume that $f \in H^{-1}(\Omega)$, where $H^{-1}(\Omega)$ is the dual space of $H^1_0(\Omega) = \widetilde{H}^1_{\Gamma,0}(\widetilde{\Omega})$. For the interface problem described by (1.1) and (1.3), we consider its weak form: find $u \in H^1(\Omega)$ such that $u = g$ on $\partial\Omega$ and

$$a(u,v) = L(v) \quad \forall\ v \in H^1_0(\Omega), \tag{2.1}$$

where

$$a(u,v) = (\beta\nabla u, \nabla v), \quad L(v) = \langle f, v\rangle_{H^{-1}(\Omega), H^1_0(\Omega)},$$

$\langle\cdot,\cdot\rangle_{V',V}$ being the duality pairing between the topological vector space V and its dual space V'. An application of Lax-Milgram Lemma shows that there exists a unique solution $u \in H^1(\Omega)$ for (2.1) such that

$$\|u\|_1 \le C\|f\|_{-1},$$

where C is a positive constant depending only on Ω and β.

2.2. Nonconforming FE functions. Let Ω be a rectangular domain or a union of rectangular domains. Without loss of generality, assume that $\{\mathcal{T}_h\}$ is a family of uniform Cartesian meshes for the domain Ω with the mesh parameter $h > 0$. For each element $T \in \mathcal{T}_h$, we call it an interface element if the interior of T intersects with the interface Γ; otherwise, we call it a non-interface element. Without loss of generality, we assume that interface elements in $\mathcal{T}_h$ satisfy the following hypotheses when the mesh size h is small enough:

(H1) The interface Γ cannot intersect an edge of any rectangular element at more than two points unless the edge is part of Γ.

(H2) If Γ intersects the boundary of a rectangular element at two points, these intersection points must be on different edges of this element.

Denote by $\mathcal{T}_h^i$ and $\mathcal{T}_h^n = \mathcal{T}_h \setminus \mathcal{T}_h^i$ the collections of all interface elements and non-interface elements, respectively. For a typical element $T = \square A_1A_2A_3A_4 \in \mathcal{T}_h$, the following conventions for its vertices and edges are assumed:

$$A_1 = (x_1, y_1), \quad A_2 = (x_1 + h, y_1), \quad A_3 = (x_1, y_1 + h), \quad A_4(x_1 + h, y_1 + h), \tag{2.2}$$

and

$$\gamma_1 = \overline{A_1A_2}, \quad \gamma_2 = \overline{A_2A_4}, \quad \gamma_3 = \overline{A_4A_3}, \quad \gamma_4 = \overline{A_3A_1}. \tag{2.3}$$

For $j = 1, 2, 3, 4$, denote by M_j the midpoint of the edge γ_j.

We follow the triplet definition of a finite element [5] to distinguish the following two finite elements introduced in [26]. The first finite element is defined by (T, Π_T, Σ_T^P), where

$$\Pi_T = \mathrm{Span}\{1, x, y, x^2 - y^2\}, \quad \Sigma_T^P = \{\psi(M_j), j = 1, 2, 3, 4 \mid \ \psi \in \Pi_T\}. \tag{2.4}$$

Here the superscript P emphasizes that the degrees of freedom are determined by the point values at the edge midpoints. Denote by $\psi_{j,T}^P$, $j = 1, 2, 3, 4$, the local basis functions such that

$$\psi_{j,T}^P(M_k) = \delta_{jk}, \quad \forall\ j, k = 1, 2, 3, 4. \tag{2.5}$$

The second finite element is defined by (T, Π_T, Σ_T^I), where

$$\Sigma_T^I = \left\{ \frac{1}{|\gamma_j|} \int_{\gamma_j} \psi \mathrm{d}s, j = 1, 2, 3, 4 \ \mid \ \psi \in \Pi_T \right\}, \tag{2.6}$$

where $|\gamma_j|$ denotes the length of the edge γ_j. The superscript I is adopted in order to emphasize that the degrees of freedom are given by the integral values over edges. The local basis functions $\psi_{j,T}^I$, $j = 1, 2, 3, 4$, fulfill

$$\frac{1}{|\gamma_k|} \int_{\gamma_k} \psi_{j,T}^I \mathrm{d}s = \delta_{jk}, \quad \forall\ j, k = 1, 2, 3, 4. \tag{2.7}$$

Set the local finite element spaces as follows

$$\mathcal{S}_h^{P,n}(T) = \mathrm{Span}\,\{\psi_{j,T}^P : j = 1, 2, 3, 4\}, \quad \mathcal{S}_h^{I,n}(T) = \mathrm{Span}\,\{\psi_{j,T}^I : j = 1, 2, 3, 4\}. \tag{2.8}$$

It is obvious that on every element $T \in \mathcal{T}_h$, $\mathcal{S}_h^{P,n}(T) = \mathcal{S}_h^{I,n}(T) = \Pi_T$. From now on, we designate by $\mathcal{S}_h^n(T)$ the local nonconforming rotated-Q_1 finite element space Π_T on an element T.

2.3. Nonconforming IFE Functions. Next, we describe the construction of a local IFE function ϕ_T^I with integral-value degrees of freedom on a typical interface element $T \in \mathcal{T}_h^i$ whose vertices and edges are given in (2.2) - (2.3). The construction of a local IFE function ϕ_T^P with midpoint-value degrees of freedom follows a similar approach.

Assume that an interface curve Γ intersects $T \in \mathcal{T}_h$ at two different points D and E, and the line segment $\overline{DE}$ separates T into two subelements T^+ and T^-. Depending on the adjacency of the edges containing D and E, the interface elements will be classified as Type I and II interface elements such that these two edges are located at two adjacent edges and at two opposite edges, respectively.

We use Type II interface element to exemplify the construction of the local IFE functions and corresponding spaces, i.e., we assume the interface points are such that

$$D = (x_1 + dh, y_1), \quad E = (x_1 + eh, y_1 + h),$$

where $d, e \in (0, 1)$. The local IFE function ϕ_T^I is defined as a piecewise rotated Q_1 polynomial as follows:

$$\phi_T^I(x,y) = \begin{cases} \phi_T^{I,+}(x,y) = c_1^+ + c_2^+ x + c_3^+ y + c_4^+(x^2 - y^2), & \text{if } (x,y) \in T^+, \\ \phi_T^{I,-}(x,y) = c_1^- + c_2^- x + c_3^- y + c_4^-(x^2 - y^2), & \text{if } (x,y) \in T^-. \end{cases} \tag{2.9}$$

The coefficients $c_j^{\pm}$ are determined by the average value on each edge γ_j:

$$\frac{1}{|\gamma_j|} \int_{\gamma_j} \phi_T^I(x,y) \mathrm{d}s = v_j, \quad j = 1, 2, 3, 4, \tag{2.10}$$

and the following interface jump conditions:
• continuity of the function on $\overline{DE}$:

$$[\phi_T^I(D)] = 0, \quad [\phi_T^I(E)] = 0, \quad c_4^+ = c_4^-. \tag{2.11}$$

• continuity of the flux:

$$\int_{\overline{DE}} [\boldsymbol{\nu}_{\overline{DE}} \cdot \beta \nabla \phi_T^I(x,y)] \mathrm{d}s = 0, \tag{2.12}$$

where $\boldsymbol{\nu}_{\overline{DE}}$ is the unit normal on $\overline{DE}$ to T^-.

Equations (2.10)–(2.12) provide eight constraints and lead to an 8×8 algebraic system $M_c \mathbf{C} = \mathbf{V}$ about the coefficients $\mathbf{C} = (c_1^-, \cdots, c_4^-, c_1^+, \cdots, c_4^+)^t$ with $\mathbf{V} = (v_1, \cdots, v_4, 0, \cdots, 0)^t$.

By direct calculations, one can verify that the matrix M_c is nonsingular for all $\beta^{\pm} > 0$ and $0 < d, e < 1$; see [29] for more details. Hence, an IFE function ϕ_T^I satisfying jump conditions (2.11) and (2.12) is uniquely determined by its integral mean values v_j over edges γ_j, $j = 1, 2, 3, 4$. For each $j = 1, 2, 3, 4$, let $\mathbf{V} = \mathbf{V}_j = (v_1, \cdots, v_4, 0, \cdots, 0)^t \in \mathbb{R}^8$ be the j-th canonical vector such that $v_j = 1$ and $v_k = 0$ for $k \neq j$. We can solve for $\mathbf{C}_j = (c_1^-, \cdots, c_4^-, c_1^+, \cdots, c_4^+)^t$ and use it in (2.9) to form the j-th nonconforming rotated-Q_1 local IFE basis function $\phi_{j,T}^I$. Figure 2.1 illustrates a comparison of a standard rotated Q_1 finite element basis function and its corresponding rotated Q_1 IFE basis functions in both Type I and Type II interface elements.

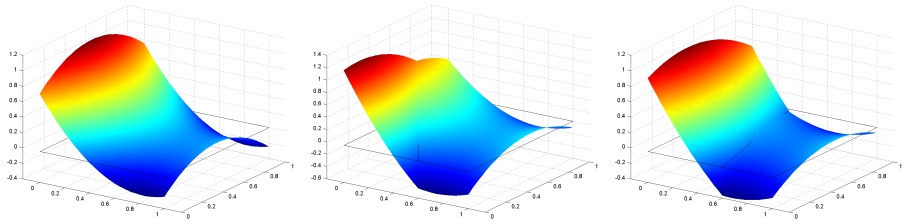

FIG. 2.1. *Nonconforming FE/IFE local bases with integral-value degrees of freedom*

The local IFE basis functions $\phi_{j,T}^P$, $j = 1, 2, 3, 4$ with midpoint-value degrees of freedom are constructed in the same procedure as those for $\phi_{j,T}^I, j = 1, 2, 3, 4$. The only modification is to replace the average value constraint (2.10) by the midpoint value constraint:

$$\phi_T^P(M_j) = v_j, \quad j = 1, 2, 3, 4, \tag{2.13}$$

where v_j are midpoint values at each edge γ_j, $j = 1, 2, 3, 4$. Choosing appropriate values of v_j, we can obtain the nodal basis functions $\phi_{j,T}^P$, $j = 1, 2, 3, 4$. An illustration of rotated-Q_1 FE/IFE local basis functions with midpoint-value degrees of freedom is provided in Figure 2.2.

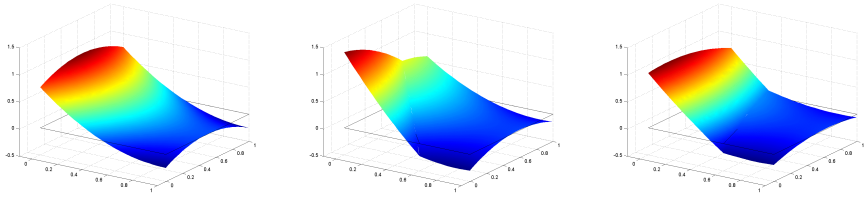

FIG. 2.2. *Nonconforming FE/IFE local basis functions with midpoint-value degrees of freedom*

Denote by

$$\mathcal{S}_h^{I,i}(T) = \text{Span}\,\{\phi_{j,T}^I : j = 1, 2, 3, 4\} \quad \text{and} \quad \mathcal{S}_h^{P,i}(T) = \text{Span}\,\{\phi_{j,T}^P : j = 1, 2, 3, 4\}$$

the local nonconforming rotated-Q_1 IFE spaces on an interface element T with integral-value and midpoint-value degrees of freedom, respectively. It is straightforward to see that $\mathcal{S}_h^{P,i}(T) = \mathcal{S}_h^{I,i}(T)$ for every $T \in \mathcal{T}_h^i$, and, from now on, we use the notation $\mathcal{S}_h^i(T)$ to denote this local IFE space on an interface element T.

Furthermore, the global IFE spaces are defined as follows

$$\begin{aligned} \mathcal{S}_h^I(\Omega) = \Big\{ & v \in L^2(\Omega) : \ v|_T \in \mathcal{S}_h^n(T) \text{ if } T \in \mathcal{T}_h^n, v|_T \in \mathcal{S}_h^i(T) \text{ if } T \in \mathcal{T}_h^i; \\ & \text{if } T_1 \cap T_2 = \gamma, \text{ then } \int_\gamma v|_{T_1}\, \mathrm{d}s = \int_\gamma v|_{T_2}\, \mathrm{d}s \Big\}, \end{aligned} \tag{2.14}$$

$$\begin{aligned} \mathcal{S}_h^P(\Omega) = \Big\{ & v \in L^2(\Omega) : \ v|_T \in \mathcal{S}_h^n(T) \text{ if } T \in \mathcal{T}_h^n, v|_T \in \mathcal{S}_h^i(T) \text{ if } T \in \mathcal{T}_h^i; \\ & \text{if } T_1 \cap T_2 = \gamma \text{ whose midpoint is } M_\gamma, \text{ then } v|_{T_1}(M_\gamma) = v|_{T_2}(M_\gamma) \Big\}. \end{aligned} \tag{2.15}$$

Notice that these two global IFE spaces are such that $\mathcal{S}_h^P(\Omega) \neq \mathcal{S}_h^I(\Omega)$ because functions in these IFE spaces have different continuity across element edges.

Depending on $T \in \mathcal{T}_h^n$ or $T \in \mathcal{T}_h^i$, we distinguish the spaces $\mathcal{S}_h^n(T)$ and $\mathcal{S}_h^i(T)$ which represent $\mathcal{S}_h^{\iota,n}(T)$ and $\mathcal{S}_h^{\iota,i}(T)$ for $\iota = P, I$.

2.4. Basic Properties of IFE Spaces. We summarize some basic and useful properties for these IFE spaces $\mathcal{S}_h^P(\Omega)$ and $\mathcal{S}_h^I(\Omega)$ in this subsection. The proofs for these properties can be found in [29].

LEMMA 2.1. **(Unisolvency)** *On each $T \in \mathcal{T}_h^i$, every IFE function $\phi_T^P \in \mathcal{S}_h^i(T)$ (resp. $\phi_T^I \in \mathcal{S}_h^i(T)$) is uniquely determined by its midpoint values* (2.13) *(resp. integral mean values* (2.10)*) and interface jump conditions* (2.11) *and* (2.12).

LEMMA 2.2. **(Continuity)** *On each $T \in \mathcal{T}_h^i$, the nonconforming local IFE space is such that $\mathcal{S}_h^i(T) \subset C(T)$.*

LEMMA 2.3. **(Partition of Unity)** *On each $T \in \mathcal{T}_h^i$, the nonconforming IFE basis functions $\phi_{i,T}^P$ and $\phi_{i,T}^I$ satisfy the partition of unity property,* i.e.,

$$\sum_{j=1}^{4} \phi_{j,T}^P(x,y) = 1, \qquad \sum_{j=1}^{4} \phi_{j,T}^I(x,y) = 1, \qquad \forall (x,y) \in T. \tag{2.16}$$

LEMMA 2.4. **(Consistency)** *On each $T \in \mathcal{T}_h^i$, IFE basis functions are consistent to standard finite element basis functions in the following sense:*

1. *If there is no jump in the coefficient, i.e., $\beta^+ = \beta^-$, then the IFE basis functions $\phi_{j,T}^P$ and $\phi_{j,T}^I$ become the standard FE basis functions $\psi_{j,T}^P$ and $\psi_{j,T}^I$, respectively.*
2. *If $\min\{|T^+|, |T^-|\}$ shrinks to zero, then the IFE basis functions $\phi_{j,T}^P$ and $\phi_{j,T}^I$ become the standard FE basis functions $\psi_{j,T}^P$ and $\psi_{j,T}^I$, respectively. Here, $|T^s|$ denotes the area of T^s, $s = +, -$.*

LEMMA 2.5. **(Flux continuity on Γ)** *On each $T \in \mathcal{T}_h^i$, every IFE function $\phi_T \in S_h^i(T)$ satisfies the flux jump condition weakly as follows*

$$\int_{\Gamma \cap T} [\boldsymbol{\nu} \cdot \beta \nabla \phi_T] ds = 0,$$

where $\boldsymbol{\nu}$ is the unit normal vector of Γ.

LEMMA 2.6. **(Boundedness)** *There exists a constant C, independent of interface location, such that for $j = 1, 2, 3, 4$, and $k = 0, 1, 2$,*

$$\|\phi_{j,T}^P\|_{k,\infty,T} \le Ch^{-k}, \quad \|\phi_{j,T}^I\|_{k,\infty,T} \le Ch^{-k}, \ \forall\ T \in \mathcal{T}_h^i. \tag{2.17}$$

THEOREM 2.7. **(Trace Inequality)** *There exists a constant $C > 0$, depending only on the diffusion coefficient β, such that*

$$\|\boldsymbol{\nu} \cdot \beta \nabla v\|_{0,\gamma} \le Ch_T^{-\frac{1}{2}} \|\sqrt{\beta} \nabla v\|_{0,T}, \ \forall\ T \in \mathcal{T}_h^i \tag{2.18}$$

for every IFE function $v \in \mathcal{S}_h^i(T)$, where γ is an edge of T, and $\boldsymbol{\nu}$ is the unit outward normal to T.

THEOREM 2.8. **(Inverse Inequality)** *There exists a constant C, depending only on the diffusion coefficient β, such that*

$$|v|_{k,\infty,T} \le Ch_T^{-1} |v|_{k,T}, \qquad |v|_{k,T} \le Ch_T^{l-k} |v|_{l,T}, \ \forall\ T \in \mathcal{T}_h^i \tag{2.19}$$

for every IFE function $v \in \mathcal{S}_h^i(T)$, and for all integers $0 \le l \le k \le 2$.

3. The Interpolation Operators and Approximation Capability. In this section, we discuss the approximation capability for nonconforming IFE spaces $\mathcal{S}_h^P(\Omega)$ and $\mathcal{S}_h^I(\Omega)$. On each non-interface element $T \in \mathcal{T}_h^n$, the local interpolation are canonically defined in two ways based on different types of degrees of freedom (2.4) and (2.6), respectively. Denote by $\mathcal{I}_T^\iota : C(\overline{T}) \to \mathcal{S}_h^n(T), \iota = P, I$, the interpolation operators with midpoint-value and integral-value degrees of freedom, respectively, such that,

$$\mathcal{I}_T^P u = \sum_{j=1}^4 u(M_j)\psi_{j,T}^P, \qquad \mathcal{I}_T^I u = \sum_{i=1}^4 \left(\frac{1}{|\gamma_i|}\int_{\gamma_i} u \ \mathrm{ds}\right)\psi_{i,T}^I, \tag{3.1}$$

where γ_j and M_j, $j = 1, 2, 3, 4$, denote the edges and the edge midpoints, respectively. The standard scaling argument leads to the following error estimates [26, Lemma 1]:

$$\|\mathcal{I}_T^\iota u - u\|_{0,T} + h|\mathcal{I}_T^\iota u - u|_{1,T} \le Ch^2|u|_{2,T}, \quad \iota = P \text{ or } I. \tag{3.2}$$

On each interface element $T \in \mathcal{T}_h^i$, the interpolation operators $\mathcal{I}_T^\iota : C(\overline{T}) \to \mathcal{S}_h^i(T), \iota = P, I$, are defined by the degrees of freedom (2.4) and (2.6), respectively. Then the local interpolation properties hold:

$$\mathcal{I}_T^P u = \sum_{j=1}^4 u(M_j)\phi_{j,T}^P, \ \ \mathcal{I}_T^I u = \sum_{i=1}^4 \left(\frac{1}{|\gamma_i|}\int_{\gamma_i} u \ \mathrm{ds}\right)\phi_{i,T}^I, \ \forall\ u \in C(\overline{T}). \tag{3.3}$$

Finally, we define the global IFE interpolation $\mathcal{I}_h^\iota : C(\overline{\Omega}) \to \mathcal{S}_h(\Omega), \iota = I, P$, piecewisely such that

$$(\mathcal{I}_h^\iota u)|_T = \mathcal{I}_T^\iota u, \quad \iota = P, I, \quad \forall\ T \in \mathcal{T}_h.$$

It is obvious that $\mathcal{I}_h^\iota \circ \mathcal{I}_h^\iota = \mathcal{I}_h^\iota, \iota = P, I$.

In what follows, we focus on the interpolation error analysis on interface elements.

3.1. Error Analysis of Interpolation on $\mathcal{S}_h^P(\Omega)$. We first consider the analysis of the nonconforming rotated Q_1 interpolation error $\mathcal{I}_T^P u - u$ with midpoint-value degrees of freedom. The error estimates can be obtained similarly as the linear and bilinear IFE interpolations [11, 18] using multi–point Taylor expansion. The proof can be found in [29, Chapter 3], and thus we only state the results.

THEOREM 3.1. *There exists a constant $C > 0$, independent of interface location, such that*

$$\|\mathcal{I}_T^P u - u\|_{0,T} + h|\mathcal{I}_T^P u - u|_{1,T} \le Ch^2\|u\|_{\widetilde{H}_\beta^2(T)} \quad \forall u \in \widetilde{H}_\beta^2(T) \tag{3.4}$$

on the interface element $T \in \mathcal{T}_h^i$.

THEOREM 3.2. *There exists a constant $C > 0$, such that we have the following interpolation error estimate:*

$$\|\mathcal{I}_h^P u - u\|_{0,\Omega} + h\left(\sum_{T\in\mathcal{T}_h} |\mathcal{I}_T^P u - u|_{1,T}^2\right)^{\frac{1}{2}} \le Ch^2\|u\|_{\widetilde{H}_\beta^2(\Omega)} \quad \forall u \in \widetilde{H}_\beta^2(\Omega). \tag{3.5}$$

3.2. Error Analysis of Interpolation on $\mathcal{S}_h^I(\Omega)$. Next, we consider the interpolation error $\mathcal{I}_T^I u - u$ with integral-value degrees of freedom on an interface element.

LEMMA 3.3. *There exists a constant $C > 0$, independent of the interface location, such that*

$$\|\phi_{j,T}^I\|_{0,T} + h^{\frac{1}{2}}\|\phi_{j,T}^I\|_{0,\partial T} + h|\phi_{j,T}^I|_{1,T} + h^{\frac{3}{2}}\|\phi_{j,T}^I\|_{1,\partial T} \le Ch, \quad j = 1,2,3,4, \tag{3.6}$$

for every interface element $T \in \mathcal{T}_h^i$.

Proof. Note that by (2.17), we obtain the following estimation

$$\|\phi_{j,T}^I\|_{k,T}^2 \le \|\phi_{j,T}^I\|_{k,\infty,T}^2 \int_T 1 \, \mathrm{dx} \le Ch^{2-2k}, \quad k = 0,1,$$
$$\|\phi_{j,T}^I\|_{k,\partial T}^2 \le \|\phi_{j,T}^I\|_{k,\infty,T}^2 \int_{\partial T} 1 \, \mathrm{ds} \le Ch^{1-2k}, \quad k = 0,1.$$

Here, we have used the fact that the size of an element is $|T| = O(h^2)$, and $|\partial T| = O(h)$. The result (3.6) follows from combining the above estimates. ∎

The interpolation $\mathcal{I}_T^I : \widetilde{H}_\beta^2(T) \to \mathcal{S}_h^I(T)$ has the following error estimate.

THEOREM 3.4. *There exists a constant $C > 0$, independent of interface location, such that*

$$\|\mathcal{I}_T^I u - u\|_{0,T} + h|\mathcal{I}_T^I u - u|_{1,T} \le Ch^2\|u\|_{\widetilde{H}_\beta^2(T)} \quad \forall u \in \widetilde{H}_\beta^2(T) \tag{3.7}$$

on every interface element $T \in \mathcal{T}_h^i$.

Proof. By the triangle inequality, we have

$$|\mathcal{I}_T^I u - u|_{k,T} \le |\mathcal{I}_T^I u - \mathcal{I}_T^P u|_{k,T} + |\mathcal{I}_T^P u - u|_{k,T}, \quad k = 0,1. \tag{3.8}$$

For every $\mathbf{x} \in T$ and $\alpha \in [\mathbb{Z}^+]^2$ with $|\alpha| \le 1$, by the Cauchy–Schwarz inequality,

$$\begin{aligned}
\left|\partial^\alpha(\mathcal{I}_T^I u(\mathbf{x}))\right| &= \left|\sum_{j=1}^4 \left(\frac{1}{|\gamma_j|}\int_{\gamma_j} u \mathrm{d}s\right)\partial^\alpha(\phi_{j,T}^I(\mathbf{x}))\right| \\
&\le \sum_{j=1}^4 \frac{1}{|\gamma_j|}\left|\int_{\gamma_j}|u|^2\mathrm{d}s\right|^{\frac{1}{2}}\left|\int_{\gamma_j} 1\mathrm{d}s\right|^{\frac{1}{2}}\left|\partial^\alpha(\phi_{j,T}^I(\mathbf{x}))\right| \\
&\le \sum_{j=1}^4 \frac{1}{|\gamma_j|^{\frac{1}{2}}}\|u\|_{0,\gamma_j}\left|\partial^\alpha(\phi_{j,T}^I(\mathbf{x}))\right|. \qquad (3.9)
\end{aligned}$$

Then, for every $u \in H^1(T)$, and $k = 0,1$, we have the following estimates by (3.6) and trace inequalities:

$$\begin{aligned}
\left|\mathcal{I}_T^I u\right|_{k,T} &\le \sum_{j=1}^4 \frac{1}{|\gamma_j|^{\frac{1}{2}}}\|u\|_{0,\gamma_j}\left|\phi_{j,T}^I\right|_{k,T} \le Ch^{1-k}\sum_{j=1}^4 \frac{1}{|\gamma_j|^{\frac{1}{2}}}\|u\|_{0,\gamma_j} \\
&\le Ch^{1-k}\sum_{j=1}^4 \frac{1}{|\gamma_j|^{\frac{1}{2}}}\left(h^{-\frac{1}{2}}\|u\|_{0,T} + h^{\frac{1}{2}}|u|_{1,T}\right) \\
&\le C\left(h^{-k}\|u\|_{0,T} + h^{1-k}|u|_{1,T}\right). \qquad (3.10)
\end{aligned}$$

Also note that

$$\mathcal{I}_T^I u - \mathcal{I}_T^P u = \mathcal{I}_T^I u - \mathcal{I}_T^I \mathcal{I}_T^P u = \mathcal{I}_T^I (u - \mathcal{I}_T^P u),$$

and $u - \mathcal{I}_T^P u \in H^1(T)$; hence, from (3.10) and (3.4) it follows that

(3.11)
$$|\mathcal{I}_T^I u - \mathcal{I}_T^P u|_{k,T} \leq C \left(h^{-k} \|u - \mathcal{I}_T^P u\|_{0,T} + h^{1-k} |u - \mathcal{I}_T^P u|_{1,T} \right) \leq C h^{2-k} \|u\|_{\widetilde{H}^2_\beta(T)}$$

Now, (3.7) follows from the combination of (3.4), (3.8), and (3.11). ∎

The global interpolation error estimate follows from combining (3.2) and (3.7) and summing over all the elements.

THEOREM 3.5. *There exists a constant $C > 0$, such that we have the following interpolation error estimate*

$$\|\mathcal{I}_h^I u - u\|_{0,\Omega} + h \left(\sum_{T \in \mathcal{T}_h} |\mathcal{I}_T^I u - u|_{1,T}^2 \right)^{\frac{1}{2}} \leq C h^2 \|u\|_{\widetilde{H}^2_\beta(\Omega)} \quad \forall u \in \widetilde{H}^2_\beta(\Omega). \tag{3.12}$$

3.3. The nonconforming IFE Galerkin method. Given a mesh $\mathcal{T}_h$, we denote by $\mathcal{E}_h$, $\mathring{\mathcal{E}}_h$ and $\mathcal{E}_h^b$ the set of its edges, interior edges, and boundary edges, respectively. The sets of interface edges and non-interface edges are denoted by $\mathcal{E}_h^i$ and $\mathcal{E}_h^n$, respectively. For the sake of simplicity, in the following discussion, we assume that the interface curve Γ does not intersect the boundary $\partial\Omega$. Consequently, $\mathcal{E}_h^b \subset \mathcal{E}_h^n$.

Define the bilinear and linear form

$$a_h(u, v) = \sum_{T \in \mathcal{T}_h} \int_T \beta \nabla u \cdot \nabla v \, \mathrm{dx}, \quad L(v) = \sum_{T \in \mathcal{T}_h} \int_T f v \, \mathrm{dx}.$$

The nonconforming IFE Galerkin method is to find $u_h^\iota \in \mathcal{S}_h^\iota(\Omega)$, $\iota = I, P$ such that

$$a_h(u_h^\iota, v_h^\iota) = L(v_h^\iota), \quad \forall \, v_h^\iota \in \mathring{\mathcal{S}}_h^\iota(\Omega), \quad \iota = I, P. \tag{3.13}$$

subject to the boundary conditions:

$$\int_\gamma u_h^I \, \mathrm{ds} = \int_\gamma g \, \mathrm{ds} \quad \text{or} \quad u_h^P(M_\gamma) = g(M_\gamma), \quad \forall \, \gamma \in \mathcal{E}_h^b, \tag{3.14}$$

where M_γ is the midpoint of γ. Here the test function spaces are defined as follows

$$\mathring{\mathcal{S}}_h^P(\Omega) = \{v \in \mathcal{S}_h^P(\Omega) : v(M_\gamma) = 0, \text{ if } \gamma \in \mathcal{E}_h^b\},$$
$$\mathring{\mathcal{S}}_h^I(\Omega) = \{v \in \mathcal{S}_h^I(\Omega) : \int_\gamma v \, \mathrm{ds} = 0, \text{ if } \gamma \in \mathcal{E}_h^b\}.$$

In the following, we derive the error estimation of IFE solutions u_h^I with integral-value degrees of freedom. Numerical examples in Section 4 will demonstrate that IFE solutions u_h^P with midpoint-value degrees of freedom do not always have optimal convergence rates.

3.4. Projection operators. For convenience in the analysis to follow, let

$$\gamma_{jk} = \partial T_j \cap \partial T_k, \quad \gamma_j = \partial T_j \cap \partial\Omega, \quad \forall\, T_j, T_k \in \mathcal{T}_h,$$

and write

$$v_j = v|_{T_j} \quad \forall\, T_j \in \mathcal{T}_h; \quad v_{jk} = v_j|_{\gamma_{jk}} \quad \forall \gamma_{jk} \in \mathcal{E}_h^i.$$

Set

$$\Lambda^h = \Big\{ \lambda \mid \lambda = (\lambda_{jk}, \lambda_{kj}) \in (\mathcal{P}_0(\gamma_{jk}))^2, \lambda_{jk} + \lambda_{kj} = 0 \ \ \forall \gamma_{jk} \in \mathring{\mathcal{E}}_h; \\ \lambda = \lambda_j \in \mathcal{P}_0(\gamma_j) \ \ \forall \gamma_j \in \mathcal{E}_h^b \Big\}.$$

Denote by $\boldsymbol{\nu}_j$ the unit outward normal to T_j. We will use the following projection operators introduced in [7]: $\Pi_0 : \underset{\gamma\in\mathcal{E}_h}{\amalg} L^2(\gamma) \to \underset{\gamma\in\mathcal{E}_h}{\amalg} \mathcal{P}_0(\gamma)$ and $\Pi_{\boldsymbol{\nu}} : \widetilde{H}^2_\beta(\Omega) \to \Lambda^h$ by

$$\langle v - \Pi_0 v, 1\rangle_\gamma = 0, \quad \forall v \in L^2(\gamma) \quad \forall \gamma \in \mathcal{E}_h, \tag{3.15}$$

$$\left\langle \beta \frac{\partial v_j}{\partial \boldsymbol{\nu}_j} - \Pi_{\boldsymbol{\nu}} v, 1 \right\rangle_{\gamma_{jk}} = 0, \quad \forall v \in \widetilde{H}^2_\beta(\Omega) \quad \forall \gamma_{jk} \in \mathcal{E}_h, \tag{3.16}$$

so that $\Pi_0^\gamma(v) := \Pi_0(v|_\gamma) = \frac{1}{|\gamma|}\int_\gamma v \, \mathrm{ds}$ is the average of v over γ and

$$\big(\Pi_{\boldsymbol{\nu}} v|_{\gamma_{jk}}, \Pi_{\boldsymbol{\nu}} v|_{\gamma_{kj}}\big) = \left(\Pi_0^{\gamma_{jk}} \beta \frac{\partial v_j}{\partial \boldsymbol{\nu}_j}, \Pi_0^{\gamma_{kj}} \beta \frac{\partial v_k}{\partial \boldsymbol{\nu}_k}\right) \in \mathbb{R}^2 \quad \forall \gamma_{jk} \in \mathcal{E}_h^i.$$

LEMMA 3.6. *Let $\gamma = (0,h)$ with $\gamma^- = (0,\alpha)$ and $\gamma^+ = (\alpha, h)$. Assume $u \in L^2(\gamma)$ and $u|_{\gamma^\iota} \in H^{\frac{1}{2}}(\gamma^\iota), \iota = -, +$. Then $u \in H^{\frac{1}{2}-\epsilon}(\gamma)$ for every $\epsilon \in (0, \frac{1}{4})$, and there exists a constant C such that*

$$\|u\|_{\frac{1}{2}-\epsilon,\gamma} \le \frac{C}{\sqrt{\epsilon}} \left(\|u\|_{\frac{1}{2},\gamma^-} + \|u\|_{\frac{1}{2},\gamma^+} \right).$$

Proof. For every $\epsilon \in (0, \frac{1}{4})$, let $\sigma = \frac{1}{2} - \epsilon$. Then $\sigma \in (\frac{1}{4}, \frac{1}{2})$. For $q \ge 1$ and $y \in \gamma^-$,

$$\int_{\gamma^+} \frac{1}{|x-y|^{(1+2\sigma)q}} dx = \frac{(h-y)^{1-(1+2\sigma)q} - (\alpha - y)^{1-(1+2\sigma)q}}{1-(1+2\sigma)q}.$$

Since $\sigma \in (\frac{1}{4}, \frac{1}{2})$, we specifically choose

$$q = \frac{1}{2}\left(1 + \frac{2}{1+2\sigma}\right), \quad \Longrightarrow \quad q = \frac{2-\epsilon}{2(1-\epsilon)}.$$

Then $1 \le q < \frac{2}{1+2\sigma}$, $1-(1+2\sigma)q \ne -1$, and $1 + 2\sigma \le (1+2\sigma)q < 2$. Hence,

$$\begin{aligned} &I(\gamma^-, \gamma^+, \sigma, q) := \int_{\gamma^-}\int_{\gamma^+} \frac{1}{|x-y|^{(1+2\sigma)q}} dxdy \\ &= \left(\frac{1}{1-(1+2\sigma)q}\right)\left(\frac{1}{2-(1+2\sigma)q}\right)\left(h^{2-(1+2\sigma)q} - (h-\alpha)^{2-(1+2\sigma)q} - \alpha^{2-(1+2\sigma)q}\right) \\ &\le C \left|\frac{1}{1-(1+2\sigma)q}\right| \left|\frac{1}{2-(1+2\sigma)q}\right| = C \left|\frac{1}{1-\epsilon}\right| \left|\frac{1}{\epsilon}\right| \le \frac{C}{\epsilon}. \end{aligned}$$

Therefore, using p such that $\frac{1}{p}+\frac{1}{q}=1$, and the above estimate, we have

$$\begin{aligned}
&\int_{\gamma^-}\int_{\gamma^+}\frac{|u(x)-u(y)|^2}{|x-y|^{1+2\sigma}}dxdy\\
&\le \int_{\gamma^-}\left(\left[\int_{\gamma^+}|u(x)-u(y)|^{2p}\,dx\right]^{\frac{1}{2p}}\right)^2\left[\int_{\gamma^+}\frac{1}{|x-y|^{(1+2\sigma)q}}dx\right]^{\frac{1}{q}}dy\\
&\le 2\int_{\gamma^-}\|u\|^2_{0,2p,\gamma^+}\left[\int_{\gamma^+}\frac{1}{|x-y|^{(1+2\sigma)q}}dx\right]^{\frac{1}{q}}dy+2\int_{\gamma^-}|u(y)|^2\left[\int_{\gamma^+}\frac{1}{|x-y|^{(1+2\sigma)q}}\,\mathrm{dx}\right]^{\frac{1}{q}}dy.\\
&\le 2\|u\|^2_{0,2p,\gamma^+}\left(\int_{\gamma^-}1^p dy\right)^{\frac{1}{p}}I(\gamma^-,\gamma^+,\sigma,q)^{\frac{1}{q}}+2\left(\int_{\gamma^-}|u(y)|^{2p}dy\right)^{\frac{1}{p}}I(\gamma^-,\gamma^+,\sigma,q)^{\frac{1}{q}}\\
&\le C\|u\|^2_{0,2p,\gamma^+}\left(\frac{1}{\epsilon}\right)^{\frac{1}{q}}+C\|u\|^2_{0,2p,\gamma^-}\left(\frac{1}{\epsilon}\right)^{\frac{1}{q}}\\
&\le C\left(\frac{1}{\epsilon}\right)^{\frac{2(1-\epsilon)}{2-\epsilon}}\left(\|u\|^2_{\frac{1}{2},\gamma^-}+\|u\|^2_{\frac{1}{2},\gamma^+}\right).
\end{aligned}$$

In the last step, we used the Sobolev embedding theorem for one dimension:

$$W^{\frac{1}{2},2}(\gamma^s)\hookrightarrow W^{0,p}(\overline{\gamma^s}),\quad s=-,+,\quad p\in[1,\infty).$$

By definition of the fractional Sobolev norm, we have

$$\begin{aligned}
\|u\|^2_{\sigma,\gamma}&=\|u\|^2_{0,\gamma}+\int_\gamma\int_\gamma\frac{|u(x)-u(y)|^2}{|x-y|^{1+2\sigma}}dxdy\\
&=\|u\|^2_{0,\gamma}+\int_{\gamma^-}\int_{\gamma^-}\frac{|u(x)-u(y)|^2}{|x-y|^{1+2\sigma}}dxdy+2\int_{\gamma^-}\int_{\gamma^+}\frac{|u(x)-u(y)|^2}{|x-y|^{1+2\sigma}}dxdy\\
&\quad+\int_{\gamma^+}\int_{\gamma^+}\frac{|u(x)-u(y)|^2}{|x-y|^{1+2\sigma}}dxdy\\
&\le\|u\|^2_{\frac{1}{2},\gamma^-}+\|u\|^2_{\frac{1}{2},\gamma^+}+C\left(\frac{1}{\epsilon}\right)^{\frac{2(1-\epsilon)}{2-\epsilon}}\left(\|u\|^2_{\frac{1}{2},\gamma^-}+\|u\|^2_{\frac{1}{2},\gamma^+}\right),
\end{aligned}$$

which leads to

$$\|u\|_{\sigma,\gamma}\le\frac{C}{\epsilon^{(1-\epsilon)/(2-\epsilon)}}\left(\|u\|_{\frac{1}{2},\gamma^-}+\|u\|_{\frac{1}{2},\gamma^+}\right)\le\frac{C}{\sqrt{\epsilon}}\left(\|u\|_{\frac{1}{2},\gamma^-}+\|u\|_{\frac{1}{2},\gamma^+}\right)$$

because for small ϵ, we have

$$\frac{1-\epsilon}{2-\epsilon}=\frac{1}{2}-\frac{\epsilon}{4}-\frac{\epsilon^2}{8}-\frac{\epsilon^3}{16}-\cdots\le\frac{1}{2}.$$

□

THEOREM 3.7. *Let $T\in\mathcal{T}_h$ and let γ be an edge of T. Then there exists a constant $C>0$ such that the following hold on a mesh $\mathcal{T}_h$ with a sufficiently small mesh size:*

1. *If $T\in\mathcal{T}_h^n$ and $v\in H^2(T)+\mathcal{S}_h^n(T)$, then*

$$\|\beta\frac{\partial v}{\partial\boldsymbol{\nu}}-\Pi_{\boldsymbol{\nu}}v\|_{0,\gamma}\le Ch^{\frac{1}{2}}\|v\|_{H^2(T)}.$$

2. If $\gamma \in \mathcal{E}_h^n$ but $T \in \mathcal{T}_h^i$, and $v \in \widetilde{H}_\beta^2(T) + \mathcal{S}_h^i(T)$, then

$$\|\beta \frac{\partial v}{\partial \boldsymbol{\nu}} - \Pi_{\boldsymbol{\nu}} v\|_{0,\gamma} \leq C h^{\frac{1}{2}} \left(\|v\|_{H^2(\widetilde{T}^-)} + \|v\|_{H^2(\widetilde{T}^+)} \right).$$

3. If $\gamma \in \mathcal{E}_h^i$ and $v \in \widetilde{H}_\beta^2(T) + \mathcal{S}_h^i(T)$, then

$$\|\beta \frac{\partial v}{\partial \boldsymbol{\nu}} - \Pi_{\boldsymbol{\nu}} v\|_{0,\gamma} \leq C h^{\frac{1}{2}} |\log h|^{\frac{1}{2}} \left(\|v\|_{H^2(\widetilde{T}^-)} + \|v\|_{H^2(\widetilde{T}^+)} \right).$$

Here, for $T \in \mathcal{T}_h^i$, designate

$$\widetilde{T}^s = \begin{cases} T \cap \Omega^s, & \text{for } v \in \widetilde{H}_\beta^2(T), \\ T^s, & \text{for } v \in \mathcal{S}_h(T), \end{cases} \qquad \text{for } s = \pm.$$

Proof. Let $\gamma \in \mathcal{E}_h$. In the first two cases we assume $\gamma \in \mathcal{E}_h^n$, but for the third case we assume $\gamma \in \mathcal{E}_h^i$. Then by the standard trace theorem or the lemma above, we have $\beta \frac{\partial v}{\partial \boldsymbol{\nu}} \in H^{\frac{1}{2}}(\gamma)$ or $\beta \frac{\partial v}{\partial \boldsymbol{\nu}} \in H^{\frac{1}{2}-\epsilon}(\gamma)$ for any $\epsilon \in (0, \frac{1}{4})$.

Since $\Pi_{\boldsymbol{\nu}} v$ is the L^2 projection of $\beta \frac{\partial v}{\partial \boldsymbol{\nu}}$ to the space of constant polynomials, applying the error estimate for polynomial projection and the standard error estimate on interpolation of Sobolev spaces (see [8, Theorem 1.4, p.6]), we have

$$\left\| \beta \frac{\partial v}{\partial \boldsymbol{\nu}} - \Pi_{\boldsymbol{\nu}} v \right\|_{0,\gamma} \leq \begin{cases} C h^{\frac{1}{2}} \left\| \beta \frac{\partial v}{\partial \boldsymbol{\nu}} \right\|_{\frac{1}{2},\gamma}, & \text{if } \gamma \in \mathcal{E}_h^n, \\ C h^{\frac{1}{2}-\epsilon} \left\| \beta \frac{\partial v}{\partial \boldsymbol{\nu}} \right\|_{\frac{1}{2}-\epsilon,\gamma}, & \text{if } \gamma \in \mathcal{E}_h^i. \end{cases} \tag{3.17}$$

For the first two cases, by the definition of $\|\cdot\|_{\frac{1}{2},\gamma}$, we have

$$\left\| \beta \frac{\partial v}{\partial \boldsymbol{\nu}} \right\|_{\frac{1}{2},\gamma} \leq \begin{cases} \left\| \beta \frac{\partial v}{\partial \boldsymbol{\nu}} \right\|_{1,T}, & \text{if } T \in \mathcal{T}_h^n, \\ \left\| \beta \frac{\partial v}{\partial \boldsymbol{\nu}} \right\|_{1,\widetilde{T}^s} \leq \left\| \beta \frac{\partial v}{\partial \boldsymbol{\nu}} \right\|_{1,\widetilde{T}^-} + \left\| \beta \frac{\partial v}{\partial \boldsymbol{\nu}} \right\|_{1,\widetilde{T}^+}, & \text{if } T \in \mathcal{T}_h^i, \end{cases}$$

which mean

$$\left\| \beta \frac{\partial v}{\partial \boldsymbol{\nu}} \right\|_{\frac{1}{2},\gamma} \leq \begin{cases} \max\{\beta^+, \beta^-\} \|v\|_{2,T}, & \text{if } T \in \mathcal{T}_h^n, \\ \max\{\beta^+, \beta^-\} \|v\|_{\widetilde{H}_\beta^2(T)}, & \text{if } T \in \mathcal{T}_h^i. \end{cases} \tag{3.18}$$

For the third case, applying Lemma 3.6, we have

$$\begin{aligned} \left\| \beta \frac{\partial v}{\partial \boldsymbol{\nu}} \right\|_{\frac{1}{2}-\epsilon,\gamma} &\leq \frac{C}{\sqrt{\epsilon}} \left(\|\beta \frac{\partial v}{\partial \boldsymbol{\nu}}\|_{\frac{1}{2},\gamma^-} + \|\beta \frac{\partial v}{\partial \boldsymbol{\nu}}\|_{\frac{1}{2},\gamma^+} \right) \\ &\leq \frac{C}{\sqrt{\epsilon}} \left(\|v\|_{2,\widetilde{T}^-} + \|v\|_{2,\widetilde{T}^+} \right). \end{aligned} \tag{3.19}$$

Finally, all the estimates in this theorem follow by applying (3.18) and (3.19) to (3.17), by taking the minimum of $\frac{1}{h^\epsilon \sqrt{\epsilon}}$ over $0 < \epsilon < 1/4$. Indeed, at $\epsilon = \frac{1}{2 \log \frac{1}{h}}$, for $0 < h < \frac{1}{e^2}$, the minimum value is

$$\frac{1}{h^\epsilon \sqrt{\epsilon}} = h^{\frac{1}{2 \log h}} \sqrt{2 \log \frac{1}{h}} = \sqrt{2e} |\log h|^{\frac{1}{2}}.$$

□

3.5. The Energy-Norm Error Estimate. Define the (broken) energy norm

$$|\!|\!| u |\!|\!| = \sqrt{a_h(u,u)}.$$

As needed, we quote the following second Strang lemma for the IFE solution:

LEMMA 3.8. *Let $u \in \widetilde{H}^1_\Gamma(\Omega)$ and $u_h^I \in \mathcal{S}_h^I(\Omega)$ be the solutions of* (2.1) *and* (3.13)*, respectively. Then,*

$$|\!|\!| u - u_h^I |\!|\!| \le C \left\{ \inf_{v_h \in \mathcal{S}_h^I(\Omega)} |\!|\!| u - v_h |\!|\!| + \sup_{w_h \in \mathcal{S}_h^I(\Omega)} \frac{|a_h(u,w_h) - L(w_h)|}{|\!|\!| w_h |\!|\!|} \right\}. \tag{3.20}$$

We are now ready to state and derive an error estimate in the energy norm.

THEOREM 3.9. *Let $u \in \widetilde{H}^2_\beta(\Omega)$ and $u_h^I \in \mathcal{S}_h^I(\Omega)$ be the solutions of* (2.1) *and* (3.13)*, respectively. Then, there exists a constant C such that*

$$|\!|\!| u - u_h^I |\!|\!| \le Ch \left[\|u\|_{\widetilde{H}^2_\beta(\Omega)} + |\log h|^{\frac{1}{2}} \sum_{T \in \mathcal{T}_h^i} \|u\|_{\widetilde{H}^2_\beta(T)} \right]. \tag{3.21}$$

If, in addition, $u \in \widetilde{W}^{2,q}_\beta(\Omega)$ for some $q > 2$, there exists $h_0 > 0$ such that, for all $0 < h < h_0$,

$$|\!|\!| u - u_h^I |\!|\!| \le Ch \Big(\|u\|_{\widetilde{H}^2_\beta(\Omega)} + \sum_{T \in \mathcal{T}_h^i} \|u\|_{\tilde{W}^{2,q}_\beta(T)} \Big). \tag{3.22}$$

Proof. We need to estimate those terms bounding $|\!|\!| u - u_h^I |\!|\!|$ in (3.20) of the Strang lemma above. By the interpolation estimate (3.12), we can estimate the first term on the right hand side of (3.20) as follows:

$$\inf_{v_h \in \mathcal{S}_h^I(\Omega)} |\!|\!| u - v_h |\!|\!| \le Ch \|u\|_{\widetilde{H}^2_\beta(\Omega)}. \tag{3.23}$$

Next, let $w_h \in \mathcal{S}_h^I(\Omega)$ be arbitrary. Then, since $u \in H^1(\Omega)$, it follows that

$$\begin{aligned} a_h(u,w_h) &= \sum_j (\beta \nabla u, \nabla w_h)_{T_j} = -\sum_j (\nabla \cdot \beta \nabla u, w_h)_{T_j} + \sum_j \left\langle \beta \frac{\partial u_j}{\partial \boldsymbol{\nu}_j}, w_h \right\rangle_{\partial T_j} \\ &= (-\nabla \cdot \beta \nabla u, w_h) + \sum_j \left\langle \beta \frac{\partial u_j}{\partial \boldsymbol{\nu}_j}, w_h \right\rangle_{\partial T_j}. \end{aligned}$$

Hence, by choosing $m_j \in \mathcal{P}_0(T_j)$ to be the the average of w_h over T_j, one sees that

$$\begin{aligned} a_h(u,w_h) - L(w_h) &= \sum_j \left\langle \beta \frac{\partial u_j}{\partial \boldsymbol{\nu}_j}, w_h \right\rangle_{\partial T_j} = \sum_j \left\langle \beta \frac{\partial u_j}{\partial \boldsymbol{\nu}_j} - \Pi_{\boldsymbol{\nu}} u_j, w_h \right\rangle_{\partial T_j} \\ &= \sum_j \left\langle \beta \frac{\partial u_j}{\partial \boldsymbol{\nu}_j} - \Pi_{\boldsymbol{\nu}} u_j, w_h - m_j \right\rangle_{\partial T_j}. \end{aligned} \tag{3.24}$$

Hence, by Theorem 3.7, the trace inequality on T_j, and the approximation capability

of m_j, we have

$$
\begin{aligned}
&|a_h(u,w_h)-L(w_h)|\\
&\le \Big(\sum_j \Big\|\beta\frac{\partial u_j}{\partial \boldsymbol{\nu}_j}-\Pi_{\boldsymbol{\nu}}u_j\Big\|^2_{0,\partial T_j}\Big)^{\frac12}\Big(\sum_j \|w_h-m_j\|^2_{0,\partial T_j}\Big)^{\frac12}\\
&\le \Big(Ch^{\frac12}\sum_{T\in\mathcal{T}_h^n}\|u\|_{2,T}+Ch^{\frac12}|\log h|^{\frac12}\sum_{T\in\mathcal{T}_h^i}\|u\|_{\widetilde{H}^2_\beta(T)}\Big)Ch^{\frac12}\Big(\sum_j\|\nabla w_h\|^2_{0,T_j}\Big)^{\frac12}\\
&\le Ch\Big(\sum_{T\in\mathcal{T}_h^n}\|u\|_{2,T}+|\log h|^{\frac12}\sum_{T\in\mathcal{T}_h^i}\|u\|_{\widetilde{H}^2_\beta(T)}\Big)|\!|\!|w_h|\!|\!|. \qquad (3.25)
\end{aligned}
$$

Then, applying (3.23) and (3.25) to (3.20) leads to (3.21).

Assume that $u\in \widetilde{W}^{2,q}_\beta(\Omega)$ for some $q>2$. Then choose p such that $\frac1p+\frac2q=1$, so that, for $T\in\mathcal{T}_h^i$

$$
\begin{aligned}
\|u\|_{\widetilde{H}^2_\beta(T)} &\le \Big(\sum_{s=\pm}\int_{T^s}\sum_{|\alpha|\le2}|D^\alpha u|^2dx\Big)^{\frac12}\le\Big(\int_T 1^p dx\Big)^{\frac{1}{2p}}\Big(\sum_{s=\pm}\int_{T^s}\Big(\sum_{|\alpha|\le2}|D^\alpha u|^2\Big)^{\frac q2}dx\Big)^{\frac1q}\\
&\le C|T|^{\frac{1}{2p}}\Big(\sum_{s=\pm}\int_{T^s}\sum_{|\alpha|\le2}|D^\alpha u|^q dx\Big)^{\frac1q}\le Ch^{\frac1p}\|u\|_{\tilde W^{2,q}_\beta(T)}.
\end{aligned}
$$

Hence, the second term in (3.21) can be bounded by

$$
|\log h|^{\frac12}\sum_{T\in\mathcal{T}_h^i}\|u\|_{\widetilde{H}^2_\beta(T)}\le C\sum_{T\in\mathcal{T}_h^i}|\log h|^{\frac12}h^{\frac1p}\|u\|_{\tilde W^{2,q}_\beta(T)}.
$$

Since $\lim_{h\to0}|\log h|^{\frac12}h^{\frac1p}=0$, there exists $h_0>0$ such that the estimate (3.22) is valid for $0<h<h_0$. This completes the proof. □

REMARK 3.1. *Indeed,* (3.21) *implies that the IFE solution converge faster than* $\mathcal{O}(h|\log h|^{\frac12})$*, since its multiplication factor,* $\sum_{T\in\mathcal{T}_h^i}\|u\|_{\widetilde{H}^2_\beta(T)}$*, goes to zero as* $h\to0$.

3.6. Duality and the L^2-Error Estimate. Let

$$
\eta_h=\mathcal{I}_h^I u-u_h^I\in\mathring{\mathcal{S}}_h^I(\Omega),
$$

and let $\psi\in\widetilde{H}^2_\beta(\Omega)$ be the solution of the dual problem:

$$
\begin{aligned}
-\nabla\cdot(\beta\nabla\psi) &= \eta_h \quad \text{in } \Omega, &(3.26a)\\
\psi &= 0 \quad \text{on } \partial\Omega. &(3.26b)
\end{aligned}
$$

Assume that the interface problem (2.1) is $\widetilde{H}^2_\beta(\Omega)$-regular so that the elliptic regularity estimate holds:

$$
\|\psi\|_{\widetilde{H}^2_\beta(\Omega)}\le C\|\eta_h\|_0. \qquad (3.27)
$$

We start from recalling the following standard estimates for the IFE interpolation $\mathcal{I}_h^I\psi$: there exists a constant C such that

$$
\begin{cases}
\|\mathcal{I}_h^I\psi\|_{2,T}\le C\,\|\psi\|_{2,T}\,, & \forall\ T\in\mathcal{T}_h^n,\\
\|\mathcal{I}_h^I\psi\|_{2,T_j^-}+\|\mathcal{I}_h^I\psi\|_{2,T_j^+}\le C\,\|\psi\|_{\widetilde{H}^2_\beta(T)}\,, & \forall\ T\in\mathcal{T}_h^i.
\end{cases} \qquad (3.28)
$$

Since $\eta_h \in \mathring{S}_h^I(\Omega)$, it follows that

$$\begin{aligned}\|\eta_h\|_0^2 &= (-\nabla\cdot\beta\nabla\psi,\eta_h) = a_h(\psi,\eta_h) - \sum_j \left\langle \beta\frac{\partial\psi_j}{\partial\boldsymbol{\nu}_j}, \eta_{h_j}\right\rangle_{\partial T_j}\\ &= a_h(\psi,\eta_h) - \sum_j \left\langle \beta\frac{\partial\psi_j}{\partial\boldsymbol{\nu}_j} - \Pi_{\boldsymbol{\nu}}\psi_j, \eta_{h_j} - q_j\right\rangle_{\partial T_j} \quad \text{for all } q_j \in \mathcal{P}_0(T_j).\end{aligned}$$

Next, for all $v_h \in \mathring{S}_h^I(\Omega)$, similarly to (3.24), we have

$$\begin{aligned}a_h(\eta_h, v_h) &= a_h(u, v_h) - a_h(u_h^I, v_h) - a_h(u - \mathcal{I}_h^I u, v_h)\\ &= \sum_j \left\langle \beta\frac{\partial u_j}{\partial\boldsymbol{\nu}_j} - \Pi_{\boldsymbol{\nu}} u_j, v_{h_j}\right\rangle_{\partial T_j} - a_h(u - \mathcal{I}_h^I u, v_h).\end{aligned}$$

Using the property $[\psi]_{\gamma_{jk}} = 0$ and recalling the definition of $\Pi_{\boldsymbol{\nu}}$, we see that

$$\left\langle \beta\frac{\partial u_j}{\partial\boldsymbol{\nu}_j} - \Pi_{\boldsymbol{\nu}} u_j, \psi_j\right\rangle_{\gamma_{jk}} + \left\langle \beta\frac{\partial u_k}{\partial\boldsymbol{\nu}_k} - \Pi_{\boldsymbol{\nu}} u_k, \psi_k\right\rangle_{\gamma_{kj}} = 0.$$

In addition, note that for $v_h \in S_h^I(\Omega)$, $-\nabla\cdot(\beta\nabla v_h) = 0$ on every $T \in \mathcal{T}_h$; hence,

$$\begin{aligned}a_h(u - \mathcal{I}_h^I u, v_h) &= \sum_j (u - \mathcal{I}_h^I u, -\nabla\cdot(\beta\nabla v_h))_{T_j} + \sum_j \left\langle u - \mathcal{I}_h^I u, \beta\frac{\partial v_h}{\partial\boldsymbol{\nu}_j}\right\rangle_{\partial T_j}\\ &= \sum_j \left\langle u - \mathcal{I}_h^I u, \beta\frac{\partial v_h}{\partial\boldsymbol{\nu}_j} - \Pi_{\boldsymbol{\nu}_j} v_h\right\rangle_{\partial T_j}.\end{aligned}$$

Therefore

$$\begin{aligned}\|\eta_h\|_0^2 &= a_h(\psi,\eta_h) - \sum_j \left\langle \beta\frac{\partial\psi_j}{\partial\boldsymbol{\nu}_j} - \Pi_{\boldsymbol{\nu}}\psi_j, \eta_{h_j} - q_j\right\rangle_{\partial T_j}\\ &= a_h(\eta_h, \psi - v_h) - a_h(u - \mathcal{I}_h^I u, v_h)\\ &\quad - \sum_j \left\langle \beta\frac{\partial\psi_j}{\partial\boldsymbol{\nu}_j} - \Pi_{\boldsymbol{\nu}}\psi_j, \eta_{h_j} - q_j\right\rangle_{\partial T_j} + \sum_j \left\langle \beta\frac{\partial u_j}{\partial\boldsymbol{\nu}_j} - \Pi_{\boldsymbol{\nu}} u_j, v_{h_j} - \psi_j\right\rangle_{\partial T_j}\\ &= a_h(\eta_h, \psi - v_h) - \sum_j \left\langle u - \mathcal{I}_h^I u, \beta\frac{\partial v_h}{\partial\boldsymbol{\nu}_j} - \Pi_{\boldsymbol{\nu}_j} v_h\right\rangle_{\partial T_j}\\ &\quad - \sum_j \left\langle \beta\frac{\partial\psi_j}{\partial\boldsymbol{\nu}_j} - \Pi_{\boldsymbol{\nu}}\psi_j, \eta_{h_j} - q_j\right\rangle_{\partial T_j} + \sum_j \left\langle \beta\frac{\partial u_j}{\partial\boldsymbol{\nu}_j} - \Pi_{\boldsymbol{\nu}} u_j, v_{h_j} - \psi_j\right\rangle_{\partial T_j}.\end{aligned} \tag{3.29}$$

With these preparations, we are ready to derive the error estimate in the L^2–norm for the IFE solution.

THEOREM 3.10. *Assume the interface problem* (2.1) *is* $\widetilde{H}_\beta^2(\Omega)$*-regular. Then, there exists a constant* C *such that the* L^2*-norm error of the IFE solution satisfies the following estimate:*

$$\|u - u_h^I\|_0 \le Ch^2\left[|\log h|^{\frac{1}{2}}\|u\|_{\widetilde{H}_\beta^2(\Omega)} + |\log h|\sum_{T\in\mathcal{T}_h^i}\|u\|_{\widetilde{H}_\beta^2(T)}\right]. \tag{3.30}$$

Proof. We proceed to estimate each term on the right hand side of (3.29). First, choose $v_h = \mathcal{I}_h^I \psi$. Then, by (3.12) and (3.27), the first term on the right-hand side of (3.29) is bounded as follows:

$$|a_h(\eta_h, \psi - v_h)| = |a_h(\eta_h, \psi - \mathcal{I}_h^I \psi)| \leq Ch |\!|\!| \eta_h |\!|\!| \|\eta_h\|_0. \tag{3.31}$$

Again, choosing $q_j \in \mathcal{P}_0(T_j)$ to be the the average of η_h over T_j, by Theorem 3.7, the trace inequality on T_j, Theorem 3.5, and (3.27), we can bound the last two terms on the right hand side of (3.29) as follows:

$$\begin{aligned}
&\Big| \sum_j \Big\langle \beta \frac{\partial \psi_j}{\partial \boldsymbol{\nu}_j} - \Pi_{\boldsymbol{\nu}} \psi_j, \eta_{h_j} - q_j \Big\rangle_{\partial T_j} \Big| + \Big| \sum_j \Big\langle \beta \frac{\partial u_j}{\partial \boldsymbol{\nu}_j} - \Pi_{\boldsymbol{\nu}} u_j, v_{h_j} - \psi_j \Big\rangle_{\partial T_j} \Big| \\
&\quad \leq Ch \Big(\sum_{T \in \mathcal{T}_h^n} \|\psi\|_{2,T} + |\log h|^{\frac{1}{2}} \sum_{T \in \mathcal{T}_h^i} \|\psi\|_{\widetilde{H}^2_\beta(T)} \Big) |\!|\!| \eta_h |\!|\!| \\
&\qquad + Ch^2 \Big(\sum_{T \in \mathcal{T}_h^n} \|u\|_{2,T} + |\log h|^{\frac{1}{2}} \sum_{T \in \mathcal{T}_h^i} \|u\|_{\widetilde{H}^2_\beta(T)} \Big) \|\psi\|_{\widetilde{H}^2_\beta(\Omega)} \\
&\quad \leq Ch \Big(|\log h|^{\frac{1}{2}} |\!|\!| \eta_h |\!|\!| + h \sum_{T \in \mathcal{T}_h^n} \|u\|_{2,T} + h |\log h|^{\frac{1}{2}} \sum_{T \in \mathcal{T}_h^i} \|u\|_{\widetilde{H}^2_\beta(T)} \Big) \|\eta_h\|_0.
\end{aligned} \tag{3.32}$$

For the second term in (3.29), by Theorem 3.5, Theorem 3.7, (3.28) and (3.27),

$$\begin{aligned}
&\Big| \sum_j \Big\langle u - \mathcal{I}_h^I u, \beta \frac{\partial v_{h_j}}{\partial \boldsymbol{\nu}_j} - \Pi_{\boldsymbol{\nu}_j} v_h \Big\rangle_{\partial T_j} \Big| \\
&\leq \Big(\sum_j \big| u - \mathcal{I}_h^I u \big|^2_{0,\partial T_j} \Big)^{\frac{1}{2}} \Big(\sum_j \Big| \beta \frac{\partial v_{h_j}}{\partial \boldsymbol{\nu}_j} - \Pi_{\boldsymbol{\nu}_j} v_h \Big|^2_{0,\partial T_j} \Big)^{\frac{1}{2}} \\
&\leq Ch^{\frac{3}{2}} \|u\|_{\widetilde{H}^2_\beta(\Omega)} \Big(h \sum_{T \in \mathcal{T}_h^n} \|v_h\|^2_{\widetilde{H}^2_\beta(T)} + h |\log h| \sum_{T \in \mathcal{T}_h^i} \big(\|v_h\|^2_{2,T^-} + \|v_h\|^2_{2,T^+} \big) \Big)^{\frac{1}{2}} \\
&\leq Ch^2 |\log h|^{\frac{1}{2}} \|u\|_{\widetilde{H}^2_\beta(\Omega)} \|\eta_h\|_0.
\end{aligned} \tag{3.33}$$

Plugging the estimates (3.31)–(3.33) in (3.29) gives

$$\begin{aligned}
\|\eta_h\|_0 &\leq Ch |\log h|^{\frac{1}{2}} |\!|\!| \eta_h |\!|\!| + Ch^2 |\log h|^{\frac{1}{2}} \|u\|_{\widetilde{H}^2_\beta(\Omega)} \\
&\leq Ch |\log h|^{\frac{1}{2}} \left(|\!|\!| \mathcal{I}_h^I u - u |\!|\!| + |\!|\!| u - u_h^I |\!|\!| \right) + Ch^2 |\log h|^{\frac{1}{2}} \|u\|_{\widetilde{H}^2_\beta(\Omega)}.
\end{aligned}$$

Finally, applying Theorem 3.5 and Theorem 3.9 to the above estimate, we arrive at the desired estimate (3.30). This completes the proof. ∎

REMARK 3.2. *Again, the estimate given in* (3.30) *suggests that the IFE solution converges in L^2-norm better than $\mathcal{O}(h^2 |\log h|)$ which is optimal sans the usual $|\log h|$ factor.*

REMARK 3.3. *An optimal rate $O(h^2)$ without $|\log h|$ factor may be obtained with slightly better regularity $u \in \tilde{W}^{2,q}_\beta(\Omega)$, $q > 2$, and the elliptic regularity assumption based on L^q-norm. In addition, the analysis requires the interpolation error estimates for IFE functions based on L^q-norm, which will be an interesting future work.*

4. Numerical Examples. In this section, we present numerical examples to demonstrate the features of these nonconforming rotated-Q_1 IFE methods for elliptic interface problems.

We test our methods with the same example as given in [11, 29]. Let $\Omega = (-1,1)^2$, and the interface curve Γ is the circle centered at the origin with radius $r_0 = \pi/6.28$, which separates the domain into two sub-domains:

$$\Omega^- = \{(x,y) \in \Omega : x^2 + y^2 < r_0^2\}, \quad \Omega^+ = \{(x,y) \in \Omega : \ x^2 + y^2 > r_0^2\}.$$

The boundary condition g and the source function f are chosen such that the exact solution is as follows:

$$u(x,y) = \begin{cases} \dfrac{r^a}{\beta^-}, & \text{if } r < r_0, \\ \dfrac{r^a}{\beta^+} + \left(\dfrac{1}{\beta^-} - \dfrac{1}{\beta^+}\right) r_0^a, & \text{if } r > r_0, \end{cases} \tag{4.1}$$

where $a = 5$, $r = \sqrt{x^2 + y^2}$. We use a family of Cartesian meshes $(\mathcal{T}_h)_{0<h<1}$, each of which consists of $N \times N$ congruent squares of size $h = 2/N$. Errors of an IFE approximation are given in L^∞, L^2, and semi H^1 norms. L^∞-norm errors are calculated using the formula:

$$\|v_h - u\|_{L^\infty} = \max_{T \in \mathcal{T}_h} \left(\max_{(x,y) \in \hat{T} \subset T} |v_h(x,y) - u(x,y)| \right), \tag{4.2}$$

where $\hat{T}$ consists of the 49 uniformly distributed points in T. The L^2 and semi H^1 norms are computed using the 9-point Gaussian quadratures.

Two different coefficient configurations are considered: one moderate jump case $(\beta^-, \beta^+) = (1, 10)$, and one large jump case $(\beta^-, \beta^+) = (1, 10000)$. The interpolation errors $\mathcal{I}_h^I u - u$ for both moderate and large coefficients jump are listed in Table 4.1 and 4.2, respectively. The interpolation errors $\mathcal{I}_h^P u - u$ for these two configurations are listed in Table 4.3 and 4.4, respectively. Data in these tables clearly show that IFE interpolations have optimally approximate rates in both L^2 and H^1 norms. Numerical results confirm our error analysis (3.5) and (3.12). Moreover, we also observe optimal convergence rates for L^∞ norm.

TABLE 4.1
Errors of IFE interpolation $u - \mathcal{I}_h^I u$ with $\beta^- = 1$, $\beta^+ = 10$

N	$\|\cdot\|_{L^\infty}$	rate	$\|\cdot\|_{L^2}$	rate	$\|\cdot\|_{H^1}$	rate
10	2.5948E−2		9.0458E−3		1.9610E−1	
20	7.3237E−3	1.8250	2.3194E−3	1.9635	9.9238E−2	0.9826
40	1.9438E−3	1.9137	5.8358E−4	1.9908	4.9913E−2	0.9914
80	5.0059E−4	1.9572	1.4637E−4	1.9953	2.5028E−2	0.9959
160	1.2701E−4	1.9787	3.6653E−5	1.9976	1.2532E−2	0.9979
320	3.1988E−5	1.9894	9.1718E−6	1.9986	6.2705E−3	0.9989
640	8.0266E−6	1.9947	2.2939E−6	1.9994	3.1363E−3	0.9995
1280	2.0101E−6	1.9975	5.7361E−7	1.9997	1.5685E−3	0.9997

Next we solve the elliptic interface problem using nonconforming Galerkin IFE scheme (3.13). For integral-value degrees of freedom, numerical errors are reported in

TABLE 4.2
Errors of IFE interpolation $u - \mathcal{I}_h^I u$ with $\beta^- = 1$, $\beta^+ = 10000$

N	$\|\cdot\|_{L^\infty}$	rate	$\|\cdot\|_{L^2}$	rate	$\|\cdot\|_{H^1}$	rate
10	$6.0241E{-3}$		$1.7879E{-3}$		$4.1565E{-2}$	
20	$2.5141E{-3}$	1.2607	$6.3808E{-4}$	1.4864	$2.7186E{-2}$	0.6125
40	$7.4878E{-4}$	1.7474	$1.6818E{-4}$	1.9237	$1.4347E{-2}$	0.9220
80	$2.0398E{-4}$	1.8761	$4.3539E{-5}$	1.9496	$7.4222E{-3}$	0.9509
160	$5.3209E{-5}$	1.9487	$1.1102E{-5}$	1.9715	$3.7778E{-3}$	0.9743
320	$1.3902E{-5}$	1.9363	$2.8079E{-6}$	1.9832	$1.9058E{-3}$	0.9872
640	$3.5127E{-6}$	1.9846	$7.0567E{-7}$	1.9924	$9.5702E{-4}$	0.9937
1280	$8.8287E{-7}$	1.9923	$1.7691E{-7}$	1.9960	$4.7959E{-4}$	0.9967

TABLE 4.3
Errors of IFE interpolation $u - \mathcal{I}_h^P u$ with $\beta^- = 1$, $\beta^+ = 10$

N	$\|\cdot\|_{L^\infty}$	rate	$\|\cdot\|_{L^2}$	rate	$\|\cdot\|_{H^1}$	rate
10	$3.1141E{-2}$		$6.7927E{-3}$		$1.9985E{-1}$	
20	$8.7089E{-3}$	1.8383	$1.7281E{-3}$	1.9748	$9.9536E{-2}$	1.0056
40	$2.3010E{-3}$	1.9202	$4.3411E{-4}$	1.9930	$4.9993E{-2}$	0.9935
80	$5.9128E{-4}$	1.9604	$1.0877E{-4}$	1.9968	$2.5050E{-2}$	0.9969
160	$1.4986E{-4}$	1.9803	$2.7227E{-5}$	1.9982	$1.2539E{-2}$	0.9985
320	$3.7721E{-5}$	1.9901	$6.8099E{-6}$	1.9993	$6.2720E{-3}$	0.9994
640	$9.4625E{-6}$	1.9951	$1.7029E{-6}$	1.9996	$3.1367E{-3}$	0.9997
1280	$2.3697E{-6}$	1.9975	$4.2579E{-7}$	1.9998	$1.5685E{-3}$	0.9999

TABLE 4.4
Errors of IFE interpolation $u - \mathcal{I}_h^P u$ with $\beta^- = 1$, $\beta^+ = 10$

N	$\|\cdot\|_{L^\infty}$	rate	$\|\cdot\|_{L^2}$	rate	$\|\cdot\|_{H^1}$	rate
10	$8.2951E{-3}$		$1.6043E{-3}$		$4.6624E{-2}$	
20	$3.3555E{-3}$	1.3057	$4.8974E{-4}$	1.7118	$2.8337E{-2}$	0.7184
40	$8.9770E{-4}$	1.9022	$1.2558E{-4}$	1.9634	$1.4709E{-2}$	0.9460
80	$2.0293E{-4}$	1.8857	$3.2030E{-5}$	1.9711	$7.5596E{-3}$	0.9603
160	$6.4204E{-5}$	1.9198	$8.1238E{-6}$	1.9792	$3.8096E{-3}$	0.9887
320	$1.6417E{-5}$	1.9675	$2.0430E{-6}$	1.9915	$1.9121E{-3}$	0.9945
640	$4.1455E{-6}$	1.9855	$5.1251E{-7}$	1.9951	$9.5868E{-4}$	0.9960
1280	$1.0438E{-6}$	1.9897	$1.2835E{-7}$	1.9975	$4.7996E{-4}$	0.9981

Tables 4.5 and 4.6, which represent the moderate coefficient jump $(\beta^-, \beta^+) = (1, 10)$, and large coefficient jump $(\beta^-, \beta^+) = (1, 10000)$. We also test the case when the coefficient are flipped, *i.e.*, $(\beta^-, \beta^+) = (10, 1)$, and $(\beta^-, \beta^+) = (10000, 1)$. Corresponding errors are reported in Tables 4.7 and 4.8. Convergence rates in semi H^1 norm and L^2 norm confirm our error analysis (3.21) and (3.30). Data in these tables also suggest that the convergence rate in L^∞ norm are approximately $O(h^2)$, which is also optimal from the point view of the degree of polynomials in constructing IFE spaces $\mathcal{S}_h^I(\Omega)$.

In comparison, for midpoint-value degrees of freedom, Galerkin solution errors are reported in Tables 4.9 and 4.10 for small and large coefficient discontinuities. Data in these tables indicate that solutions cannot achieve optimal rates of convergence in any of L^∞, L^2, or semi H^1 norms. We observe that convergence rates for larger

TABLE 4.5
Errors of Galerkin IFE solutions $u - u_h^I$ with $\beta^- = 1$, $\beta^+ = 10$

N	$\|\cdot\|_{L^\infty}$	rate	$\|\cdot\|_{L^2}$	rate	$\|\cdot\|_{H^1}$	rate
10	$2.6183E{-2}$		$1.1395E{-2}$		$1.9585E{-1}$	
20	$7.3444E{-3}$	1.8339	$2.9860E{-3}$	1.9321	$9.9065E{-2}$	0.9833
40	$1.9455E{-3}$	1.9165	$7.4374E{-4}$	2.0054	$4.9894E{-2}$	0.9895
80	$5.0072E{-4}$	1.9580	$1.8547E{-4}$	2.0036	$2.5026E{-2}$	0.9955
160	$1.2702E{-4}$	1.9789	$4.6313E{-5}$	2.0017	$1.2531E{-2}$	0.9979
320	$3.1989E{-5}$	1.9894	$1.1671E{-5}$	1.9885	$6.2702E{-3}$	0.9990
640	$8.0267E{-6}$	1.9947	$2.9122E{-6}$	2.0027	$3.1363E{-3}$	0.9995
1280	$2.0101E{-6}$	1.9975	$7.2684E{-7}$	2.0024	$1.5684E{-3}$	0.9997

TABLE 4.6
Errors of Galerkin IFE solutions $u - u_h^I$ with $\beta^- = 1$, $\beta^+ = 10000$

N	$\|\cdot\|_{L^\infty}$	rate	$\|\cdot\|_{L^2}$	rate	$\|\cdot\|_{H^1}$	rate
10	$5.9646E{-3}$		$2.7360E{-3}$		$4.0678E{-2}$	
20	$2.5455E{-3}$	1.2285	$1.0526E{-3}$	1.3782	$2.7824E{-2}$	0.5479
40	$7.1692E{-4}$	1.8281	$2.5767E{-4}$	2.0303	$1.4700E{-2}$	0.9205
80	$2.1533E{-4}$	1.7353	$6.3614E{-5}$	2.0181	$7.5491E{-3}$	0.9614
160	$5.9653E{-5}$	1.8519	$1.5531E{-5}$	2.0342	$3.7978E{-3}$	0.9911
320	$1.5521E{-5}$	1.9423	$4.0823E{-6}$	1.9277	$1.9146E{-3}$	0.9881
640	$4.1575E{-6}$	1.9005	$1.0069E{-6}$	2.0194	$9.5881E{-4}$	0.9977
1280	$1.0588E{-6}$	1.9733	$2.4921E{-7}$	2.0145	$4.8004E{-4}$	0.9981

TABLE 4.7
Errors of Galerkin IFE solutions $u - u_h^I$ with $\beta^- = 10$, $\beta^+ = 1$

N	$\|\cdot\|_{L^\infty}$	rate	$\|\cdot\|_{L^2}$	rate	$\|\cdot\|_{H^1}$	rate
10	$2.5249E{-2}$		$1.0347E{-1}$		$1.8872E{-0}$	
20	$6.1647E{-3}$	2.0341	$2.6094E{-2}$	1.9874	$9.5266E{-1}$	0.9862
40	$1.5899E{-3}$	1.9551	$6.5402E{-3}$	1.9963	$4.7745E{-1}$	0.9966
80	$4.0597E{-4}$	1.9695	$1.6363E{-3}$	1.9989	$2.3887E{-1}$	0.9991
160	$1.0382E{-4}$	1.9673	$4.0917E{-4}$	1.9997	$1.1945E{-1}$	0.9998
320	$2.6221E{-5}$	1.9853	$1.0227E{-4}$	2.0003	$5.9730E{-2}$	0.9999
640	$6.6006E{-6}$	1.9900	$2.5570E{-5}$	1.9998	$2.9865E{-2}$	1.0000
1280	$1.6613E{-6}$	1.9903	$6.3931E{-6}$	1.9999	$1.4933E{-2}$	1.0000

coefficient jump case is lower than the small coefficient jump. In addition, convergence rates are oscillating as we uniformly refine the solution mesh which indicates that the Galerkin scheme using midpoint-value degrees of freedom is sensitive to the material configuration in the interface elements and the ratio of coefficient jumps.

We also compare the point-wise error $e_h^P(x,y) = |u_h^P(x,y) - u(x,y)|$ and $e_h^I(x,y) = |u_h^I(x,y) - u(x,y)|$ for every point $(x,y) \in \Omega$ on the same mesh containing 160×160 elements. Error functions of these two solutions are plotted in Figure 4.1. It can be observed from the left plot that the point-wise accuracy of solution u_h^I around interface are comparable to errors far away from the interface. On the other hand, the plot on the right suggests that the point-wise accuracy of u_h^P is quite poor around the interface. We suspect the reason for poor accuracy around interface is because the

TABLE 4.8
Errors of Galerkin IFE solutions $u - u_h^I$ with $\beta^- = 10000$, $\beta^+ = 1$

N	$\|\cdot\|_{L^\infty}$	rate	$\|\cdot\|_{L^2}$	rate	$\|\cdot\|_{H^1}$	rate
10	$2.5887E{-2}$		$1.0332E{-1}$		$1.8874E{-0}$	
20	$9.0928E{-3}$	1.5094	$2.6085E{-2}$	1.9858	$9.5275E{-1}$	0.9862
40	$2.2570E{-3}$	2.0144	$6.5319E{-3}$	1.9977	$4.7747E{-1}$	0.9967
80	$5.1846E{-4}$	2.1180	$1.6345E{-3}$	1.9987	$2.3887E{-1}$	0.9992
160	$1.3253E{-4}$	1.9679	$4.0880E{-4}$	1.9994	$1.1945E{-1}$	0.9998
320	$3.1459E{-5}$	2.0748	$1.0219E{-4}$	2.0002	$5.9729E{-2}$	0.9999
640	$7.7833E{-6}$	2.0150	$2.5551E{-5}$	1.9998	$2.9865E{-2}$	1.0000
1280	$1.9252E{-6}$	2.1504	$6.3885E{-6}$	1.9998	$1.4933E{-2}$	1.0000

TABLE 4.9
Errors of Galerkin IFE solutions $u - u_h^P$ with $\beta^- = 1$, $\beta^+ = 10$

N	$\|\cdot\|_{L^\infty}$	rate	$\|\cdot\|_{L^2}$	rate	$\|\cdot\|_{H^1}$	rate
10	$3.0783E{-2}$		$7.8310E{-3}$		$1.9616E{-1}$	
20	$8.6352E{-3}$	1.8338	$2.0989E{-3}$	1.8995	$9.9802E{-2}$	0.9749
40	$2.2891E{-3}$	1.9155	$5.1366E{-4}$	2.0308	$5.0359E{-2}$	0.9868
80	$7.7107E{-4}$	1.5698	$1.2297E{-4}$	2.0626	$2.5424E{-2}$	0.9860
160	$6.9062E{-4}$	0.1590	$3.0853E{-5}$	1.9948	$1.3174E{-2}$	0.9485
320	$2.8466E{-4}$	1.2787	$7.5130E{-6}$	2.0379	$6.5827E{-3}$	1.0009
640	$1.4840E{-4}$	0.9398	$3.4099E{-6}$	1.3006	$3.4749E{-3}$	0.9217
1280	$1.0162E{-4}$	0.5463	$1.6648E{-6}$	0.8734	$1.9224E{-3}$	0.8541

discontinuity of IFE functions across interface could be large for certain configurations of the interface location and diffusion coefficients.

FIG. 4.1. *Point-wise error comparison of u_h^I and u_h^P.*

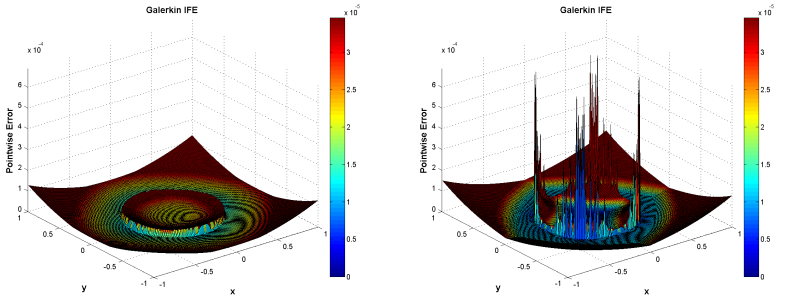

Finally, we take a closer look of the rotated Q_1 IFE functions and bilinear IFE functions [11]. In Figure 4.2, we plot the global bases of Q_1 and RQ_1 IFE function on two adjacent elements. In the left plot, there is a large gap on common interface edge of a bilinear IFE basis, where the continuity is only enforced at two endpoints of that edge. To see it more clearly, in the right plot, the traces of this bilinear IFE function are plotted in blue curves which indicate that the largest discontinuity occurs at the intersection point of the edge and the interface. On the other hand, the middle plot shows that the discontinuity of a RQ_1 IFE basis is scatter throughout the interface

TABLE 4.10
Errors of Galerkin IFE solutions $u - u_h^P$ with $\beta^- = 1$, $\beta^+ = 10000$

N	$\|\cdot\|_{L^\infty}$	rate	$\|\cdot\|_{L^2}$	rate	$\|\cdot\|_{H^1}$	rate
10	$1.0989E{-2}$		$1.8206E{-3}$		$5.5161E{-2}$	
20	$2.3770E{-3}$	2.2088	$1.0362E{-3}$	0.8130	$2.7972E{-2}$	0.9797
40	$2.3041E{-3}$	0.4502	$1.9855E{-4}$	2.3838	$1.7028E{-2}$	0.7161
80	$1.5870E{-3}$	0.5378	$4.3549E{-5}$	2.1887	$1.0654E{-2}$	0.6765
160	$1.2245E{-3}$	0.3742	$3.0930E{-5}$	0.4947	$7.4014E{-3}$	0.5256
320	$4.4228E{-4}$	1.4692	$7.6253E{-6}$	2.0201	$3.7077E{-3}$	0.9973
640	$2.8305E{-4}$	0.6439	$6.5803E{-6}$	0.2126	$2.8632E{-3}$	0.3728
1280	$1.8823E{-4}$	0.5885	$3.4795E{-6}$	0.9193	$1.9941E{-3}$	0.5220

TABLE 4.11
Errors of SPPG IFE solutions $u - u_h^P$ with $\beta^- = 1$, $\beta^+ = 10$.

N	$\|\cdot\|_{L^\infty}$	rate	$\|\cdot\|_{L^2}$	rate	$\|\cdot\|_{H^1}$	rate
10	$3.0780E{-2}$		$7.6671E{-3}$		$1.9716E{-1}$	
20	$8.6341E{-3}$	1.8338	$2.0929E{-3}$	1.8732	$1.0026E{-1}$	0.9756
40	$2.2891E{-3}$	1.9153	$5.2161E{-4}$	2.0045	$5.0424E{-2}$	0.9916
80	$5.8956E{-4}$	1.9571	$1.2971E{-4}$	2.0076	$2.5275E{-2}$	0.9964
160	$1.4962E{-4}$	1.9783	$3.2259E{-5}$	2.0075	$1.2652E{-2}$	0.9984
320	$3.7691E{-5}$	1.9891	$8.1360E{-6}$	1.9873	$6.3327E{-3}$	0.9985
640	$9.4586E{-6}$	1.9945	$2.0047E{-6}$	2.0210	$3.1684E{-3}$	0.9991
1280	$4.2436E{-6}$	1.1563	$4.8937E{-7}$	2.0344	$1.5863E{-3}$	0.9981

edge and it is less prominent. In fact, the RQ_1 basis is weakly continuous across the edge in the sense that the mean values of the two traces are exactly the same. The traces of this RQ_1 IFE function are plotted in red curves which also demonstrate a smaller discontinuity across the interface edge.

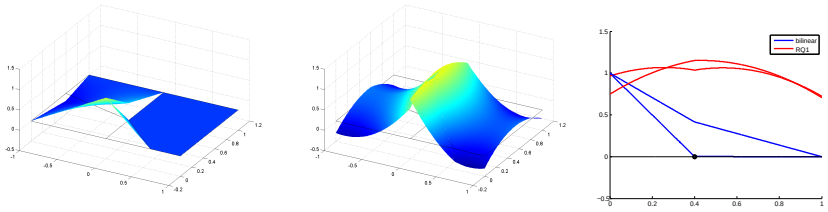

FIG. 4.2. *Comparison of bilinear and RQ_1 IFE global basis functions with $\beta^- = 1$, $\beta^+ = 1000$.*

5. Conclusions. In this article, we develop two types of rotated-Q_1 nonconforming IFE spaces based on the different types of degrees of freedom to solve elliptic interface problems. Both of these IFE spaces are proved to have optimal approximation capabilities. Error analysis of the Galerkin IFE solutions using integral-value degrees of freedom shows the optimal convergence rates.

REFERENCES

[1] I. Babuška. The finite element method for elliptic equations with discontinuous coefficients. *Computing (Arch. Elektron. Rechnen)*, 5:207–213, 1970.

[2] Z. Chen and P. Oswald. Multigrid and multilevel methods for nonconforming Q_1 elements. *Math. Comp.*, 67(222):667–693, 1998.

[3] Z. Chen and J. Zou. Finite element methods and their convergence for elliptic and parabolic interface problems. *Numer. Math.*, 79(2):175–202, 1998.

[4] S.-H. Chou, D. Y. Kwak, and K. T. Wee. Optimal convergence analysis of an immersed interface finite element method. *Adv. Comput. Math.*, 33(2):149–168, 2010.

[5] P. G. Ciarlet. *The finite element method for elliptic problems*. North-Holland Publishing Co., Amsterdam-New York-Oxford, 1978. Studies in Mathematics and its Applications, Vol. 4.

[6] M. Crouzeix and P.-A. Raviart. Conforming and nonconforming finite element methods for solving the stationary Stokes equations. I. *Rev. Française Automat. Informat. Recherche Opérationnelle Sér. Rouge*, 7(R-3):33–75, 1973.

[7] J. Douglas, Jr., J. E. Santos, D. Sheen, and X. Ye. Nonconforming Galerkin methods based on quadrilateral elements for second order elliptic problems. *M2AN Math. Model. Numer. Anal.*, 33(4):747–770, 1999.

[8] V. Girault and P.-A. Raviart. *Finite element methods for Navier-Stokes equations*, volume 5 of *Springer Series in Computational Mathematics*. Springer-Verlag, Berlin, 1986. Theory and algorithms.

[9] Y. Gong, B. Li, and Z. Li. Immersed-interface finite-element methods for elliptic interface problems with nonhomogeneous jump conditions. *SIAM J. Numer. Anal.*, 46(1):472–495, 2007/08.

[10] J. Guzman, M. A. Sanchez, and M. Sarkis. A finite element method for high-contrast interface problems with error estimates independent of contrast. *arXiv:1507.03873*, 2015.

[11] X. He, T. Lin, and Y. Lin. Approximation capability of a bilinear immersed finite element space. *Numer. Methods Partial Differential Equations*, 24(5):1265–1300, 2008.

[12] X. He, T. Lin, Y. Lin, and X. Zhang. Immersed finite element methods for parabolic equations with moving interface. *Numer. Methods Partial Differential Equations*, 29(2):619–646, 2013.

[13] H. Ji, J. Chen, and Z. Li. A symmetric and consistent immersed finite element method for interface problems. *J. Sci. Comput.*, 61(3):533–557, 2014.

[14] R. Kafafy, T. Lin, Y. Lin, and J. Wang. Three-dimensional immersed finite element methods for electric field simulation in composite materials. *Internat. J. Numer. Methods Engrg.*, 64(7):940–972, 2005.

[15] R. Kafafy and J. Wang. Whole ion optics gridlet simulations using a hybrid-grid immersed-finite-element particle-in-cell code. *J. Propulsion Power*, 23(1):59–68, 2007.

[16] P. Klouček, B. Li, and M. Luskin. Analysis of a class of nonconforming finite elements for crystalline microstructures. *Math. Comp.*, 65(215):1111–1135, 1996.

[17] D. Y. Kwak, K. T. Wee, and K. S. Chang. An analysis of a broken P_1-nonconforming finite element method for interface problems. *SIAM J. Numer. Anal.*, 48(6):2117–2134, 2010.

[18] Z. Li, T. Lin, Y. Lin, and R. C. Rogers. An immersed finite element space and its approximation capability. *Numer. Methods Partial Differential Equations*, 20(3):338–367, 2004.

[19] Z. Li, T. Lin, and X. Wu. New Cartesian grid methods for interface problems using the finite element formulation. *Numer. Math.*, 96(1):61–98, 2003.

[20] T. Lin, Y. Lin, and X. Zhang. A method of lines based on immersed finite elements for parabolic moving interface problems. *Adv. Appl. Math. Mech.*, 5(4):548–568, 2013.

[21] T. Lin, Y. Lin, and X. Zhang. Partially penalized immersed finite element methods for elliptic interface problems. *SIAM J. Numer. Anal.*, 53(2):1121–1144, 2015.

[22] T. Lin, D. Sheen, and X. Zhang. A locking-free immersed finite element method for planar elasticity interface problems. *J. Comput. Phys.*, 247:228–247, 2013.

[23] T. Lin, Q. Yang, and X. Zhang. *A Priori* error estimates for some discontinuous Galerkin immersed finite element methods. *J. Sci. Comput.*, 2015. in press.

[24] T. Lin, Q. Yang, and X. Zhang. Partially penalized immersed finite element methods for parabolic interface problems. *Numer. Methods Partial Differential Equations*, 31(6):1925–1947, 2015.

[25] T. Lin and X. Zhang. Linear and bilinear immersed finite elements for planar elasticity interface problems. *J. Comput. Appl. Math.*, 236(18):4681–4699, 2012.

[26] R. Rannacher and S. Turek. Simple nonconforming quadrilateral Stokes element. *Numer. Methods Partial Differential Equations*, 8(2):97–111, 1992.

[27] B. Rivière. *Discontinuous Galerkin methods for solving elliptic and parabolic equations*, volume 35 of *Frontiers in Applied Mathematics*. Society for Industrial and Applied Mathematics (SIAM), Philadelphia, PA, 2008. Theory and implementation.

[28] S. Vallaghé and T. Papadopoulo. A trilinear immersed finite element method for solving the electroencephalography forward problem. *SIAM J. Sci. Comput.*, 32(4):2379–2394, 2010.
[29] X. Zhang. *Nonconforming Immersed Finite Element Methods for Interface Problems*. 2013. Thesis (Ph.D.)–Virginia Polytechnic Institute and State University.